Spin and charge transport induced by a twisted light beam on the surface of a topological insulator

Kunitaka Shintani, Katsuhisa Taguchi,[*] Yukio Tanaka, and Yuki Kawaguchi

Department of Applied Physics, Nagoya University, Nagoya, 464-8603, Japan

(Received 31 December 2015; revised manuscript received 12 April 2016; published 11 May 2016)

We theoretically study spin and charge transport induced by a twisted light beam irradiated on a disordered surface of a doped three-dimensional topological insulator (TI). We find that various types of spin vortices are imprinted on the surface of the TI depending on the spin and orbital angular momentum of the incident light. The key mechanism for the appearance of the unconventional spin structure is the spin-momentum locking in the surface state of the TI. Besides, the diffusive transport of electrons under an inhomogeneous electric field causes a gradient of the charge density, which then induces nonlocal charge current and spin density as well as the spin current. We discuss the relation between these quantities within the linear response to the applied electric field using the Keldysh-Green's function method.

I. INTRODUCTION

Emergence and manipulation of spins are a major research topic in spintronics. Applying a controlled light is one of the promising techniques to manipulate spins. Recently, the spin angular momentum of a circularly polarized light has been observed to induce the magnetization in solid-state materials through spin-orbit interactions [1–4]. This technique has further been applied to the ultrafast magnetization switching, whose time is much shorter than that by an applied magnetic field [5,6].

When a light is irradiated on a surface of a three-dimensional topological insulator (TI), spin is predicted to emerge in the perpendicular direction to the electric field of the light [7–9]. Here, a TI is an anomalous material with strong spin-orbit interactions. Electrons insulate in the bulk, while they conduct on the surface of the TI, where the exotic surface state of the TI is caused by both the spin-orbit interaction and the topological electric structure [10–12]. On the surface of the TI, the direction of the spin and that of the momentum are perfectly locked to be perpendicular to each other, which is dubbed spin-momentum locking. Because of this spin-momentum locking, the charge current generated along the direction of the electric field causes the spin density in the perpendicular direction [7–9]. Such a manipulation of spin and charge current using a light may make it possible to develop magneto-optical devices based on TIs [7–9,13,14].

Recently, magneto-optical effects and optical excitation using a twisted light beam, whose phase is twisted around the direction of the propagation of light, have been theoretically predicted [15–20] and experimentally carried out [21,22]. A twisted light has the following two intriguing properties distinct from a plane wave [23]. First, the phase of the light is twisted around the center of the beam and, hence, has a singularity at the center. As a result, strength of the light becomes zero at the center of the beam. Second, because of the twisted phase, the strength of the light strongly depends on the space, whose distributions are manipulated by the angular momentum of the light. The above properties

can be well understood by writing the electric field of the light. The electric field of the twisted light beam traveling along the z axis at $z = z_0$, $\boldsymbol{E} = (E_x, E_y)$, can be described by [23–28]

$$\boldsymbol{E}(r,\varphi,t,z_0) = \mathcal{E}(r,z_0)\mathrm{Re}\big[\big(1, i\sigma_{\mathrm{L}}^z\big)e^{i(q_z z_0 - \Omega t)}e^{im_{\mathrm{L}}^z\varphi}\big], \quad (1)$$

where (r,φ) is the two-dimensional polar coordinates at $z = z_0$, t is the time, and q_z and Ω are the momentum and frequency of the twisted light beam, respectively. Here, $\mathcal{E}(r,z_0)$ denotes the magnitude of the electric field, which depends on the space and becomes zero at the center $r = 0$ for a nonzero m_{L}^z due to the phase singularity. $\sigma_{\mathrm{L}}^z = 1, -1$ and $m_{\mathrm{L}}^z = 0, \pm 1, \pm 2, \ldots$ represent the z components of the spin and orbital angular momentum of the light, respectively. The former corresponds to the direction of the circular polarization, i.e., $\sigma_{\mathrm{L}}^z = 1(-1)$ represents a right-handed (left-handed) circularly polarized wave, while the latter describes the winding of the electric field in the $z = z_0$ plane. In fact, the electric field of a twisted light has the topological quantity. We will see later that the winding number of a twisted light given by Eq. (1) is proportional to σ_{L}^z and m_{L}^z [see the discussion below Eq. (67)].

So far, it has been theoretically predicted that in the presence of the spin-orbit interaction, unconventional photoinduced spin excitation and electric current emerge due to the spatial dependence of the strength of the electric field of the twisted light. It is expected that the interband excitation can be influenced by not only the spin angular momentum, but also the orbital angular momentum of the twisted beam. However, the latter effect has not been observed so far. Actually, the experimental investigation of the photoinduced spin polarization [22] could not detect the orbital angular momentum dependence in the semiconductor with the Rashba- and Dresselhaus-type spin-orbit interactions. There is a theoretical prediction that the orbital angular momentum dependence can be observed in cylindrical quantum disks [15].

In this paper, we theoretically study spin and charge generation due to the electric field of the twisted light beam on a disordered surface of a doped TI by using the Green's function technique. We analytically calculate the linear response function of the spin density to a space-time-dependent

---
[*]taguchi@rover.nuap.nagoya-u.ac.jp

external electric field. We find that the local and nonlocal spin densities are induced by the electric field and the gradient of the electric field, respectively, via the spin-momentum locking. Here, the local spin density comes from the charge current that flows along the electric field, whereas the nonlocal one couples to the diffusive charge current due to the impurity scatterings on the disordered surface of the TI. In addition, the gradient of the electric field also induces the charge density and the spin current. Applying the obtained results to the electric field of a twisted light beam, we find that various spin distributions appear depending on the orbital as well as spin angular momentum of the light. Moreover, the spin distributions have topological structures, i.e., magnetic vortexlike textures, characterized with winding numbers, which depend on both σ_L^z and m_L^z. The induced spin structure evolves in time but its winding number remains a constant. The manipulation of such a topological spin structure could be applicable for the spintronics related to magnetic vortices and skyrmions.

This paper is organized as follows. In Sec. II, we introduce the model Hamiltonian for the disordered surface of the TI in the presence of a space-time-dependent electromagnetic field. We also present the Green's functions on the disordered surface of the TI. In Sec. III, we calculate the response function on the surface of the TI within the linear response to the applied electric field. Readers who are interested only in the physical meaning of the responses can skip Sec. III. Section IV discusses the main results of the responses [Eqs. (39), (46), and (48)], e.g., general properties of the charge density, spin density, charge current, and spin current induced by the electric field on the surface of the TI. Section V discusses the properties of the twisted light induced spin and charge distributions. Section VI summarizes the paper. Appendixes A and B–H give the detailed calculations used in Secs. II and III, respectively.

II. MODEL

In this paper, we consider a high-quality TI such as $Bi_{1.5}Sb_{0.5}Te_{1.7}Se_{1.3}$, namely, the Fermi level is assumed to be located between the valance and conduction bands of the bulk TI [29] as schematically illustrated in Fig. 1(a). In such a high-quality TI, only the electrons at the surface contribute to the transport and the bulk is an ideal insulator. In the surface state, the spin and momentum are perfectly locked. The low-energy effective Hamiltonian describing the electrons in the surface states has been theoretically derived and experimentally demonstrated [10–12] as

$$\mathcal{H}_{TI} = \int d\boldsymbol{x}\, \psi^\dagger [-i\hbar v_F (\hat{\boldsymbol{\sigma}} \times \boldsymbol{\nabla})_z - \epsilon_F] \psi, \qquad (2)$$

where $\psi^\dagger \equiv \psi^\dagger(\boldsymbol{x}, t) = (\psi_\uparrow^\dagger\ \psi_\downarrow^\dagger)$ and ψ are the creation and annihilation operators of conduction electrons on the surface of the TI, $\hat{\sigma}_{j(=x,y,z)}$ are the Pauli matrices, and $e < 0$ is the elementary charge of electrons. Here, we assume a doped TI, and ϵ_F and v_F are the Fermi energy and the Fermi velocity, respectively, on the surface of the doped TI. We further take into account nonmagnetic impurities on the surface of the TI as
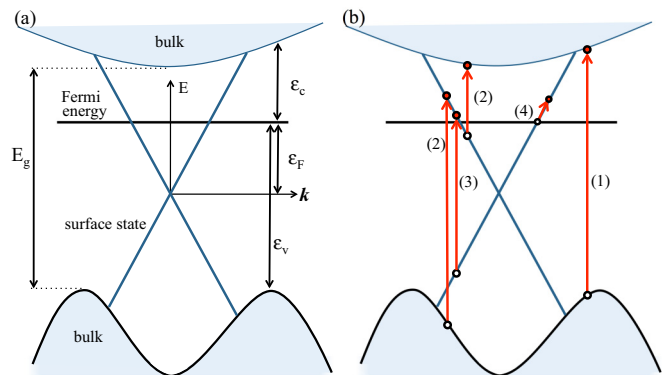

FIG. 1. (a) Schematic illustration of energy band of topological insulator and (b) processes of optical transitions: (1) interband transition from the valence band to the conduction band in the bulk TI, (2) interband transition from a surface state to a bulk energy band of the TI and vice versa, and (3) interband transition from a surface state to the other surface state with opposite helicity. This paper considers only (4) intraband excitation near the Fermi surface (see text).

well as an applied electromagnetic field. The total Hamiltonian is given by

$$\mathcal{H} = \mathcal{H}_{TI} + \mathcal{H}_{em} + \mathcal{V}_{imp}, \qquad (3)$$

$$\mathcal{H}_{em} = -ev_F \int d\boldsymbol{x}\, \psi^\dagger (\hat{\boldsymbol{\sigma}} \times \boldsymbol{A}_{em})_z \psi, \qquad (4)$$

$$\mathcal{V}_{imp} = \int d\boldsymbol{x}\, u_i \psi^\dagger \psi. \qquad (5)$$

Here, $\mathcal{H}_{em}$ is the gauge coupling between conduction electrons and the electromagnetic field. The vector potential of the electromagnetic field $\boldsymbol{A}_{em}$ generally depends on the space and time, and the electric field and the magnetic field are, respectively, given by $\boldsymbol{E} = -\partial_t \boldsymbol{A}_{em}$ and $\boldsymbol{B} = \boldsymbol{\nabla} \times \boldsymbol{A}_{em}$. $\mathcal{V}_{imp}$ in Eq. (5) describes the potential due to the nonmagnetic impurity scatterings [8,30–33], where $u_i(\boldsymbol{x}) = \sum_{j=1}^{N_i} u_0 [\delta(\boldsymbol{x} - \boldsymbol{R}_j) - \frac{1}{L^2}]$ is the potential energy density with N_i being the number of the impurities, u_0 a constant, $\boldsymbol{R}_j$ the position of the jth impurity on the surface, and L^2 the area of the surface. Here, the contribution from the impurity potential is treated as the impurity average $\langle u_i(\boldsymbol{q})u_i(\boldsymbol{q}')\rangle_i = \frac{N_i u_0^2}{L^4}\delta_{q,q'}$, where $u_i(\boldsymbol{q})$ is the Fourier transform of $u_i(\boldsymbol{x})$. Because the electrons that contribute to transport exist at the surface of the TI, whose wave function spreads over a few unit cells from the surface [34], we take account of impurities only at the surface, i.e., impurities existing within a few unit cells from the surface. Moreover, since the metallic surface states at the Fermi level are energetically well separated from the bulk conduction and valence bands, impurity scattering occurs within the surface states as described by Eq. (5) [8,30–32].

Figure 1 shows a schematic illustration of the energy band of the TI and the possible optical transition processes. Among the three interband transitions (1)–(3) and one intraband transition (4) shown in Fig. 1(b), this paper takes account of only the process (4). This is because we are considering to apply a terahertz beam [35], whose energy is in the order of a few meV. By contrast to this, in the case of $Bi_{1.5}Sb_{0.5}Te_{1.7}Se_{1.3}$,

for example, the bulk energy gap and the Fermi energy measured from the Dirac point are, respectively, given by $E_g \sim$ 0.3 eV [12] and $\epsilon_F \sim 0.2$ eV [29]. Since the characteristic energies required for the transition processes (1)–(3) are (1) E_g, (2) $\epsilon_v \sim E_g/2 + \epsilon_F$ and $\epsilon_c \sim E_g/2 - \epsilon_F$, and (3) $2\epsilon_F$, the low-energy incident light ($\hbar\Omega \sim$ a few meV) cannot excite any of the interband transitions (1)–(3).

To calculate the spin density and the charge density, we use the Green's function method. In the absence of the electromagnetic field, the retarded Green's function is given by [30,31,36]

$$\hat{g}^{\mathrm{r}}_{\boldsymbol{k},\omega} = [\hbar\omega + \epsilon_F - \hbar v_F \hat{\boldsymbol{\sigma}} \cdot (\boldsymbol{k} \times \boldsymbol{z}) - \hat{\Sigma}_{\boldsymbol{k},\omega}]^{-1}. \quad (6)$$

Here, a variable with a hat denotes a 2×2 matrix. By calculating the self-energy $\hat{\Sigma}_{\boldsymbol{k},\omega}$ within the self-consistent Born approximation [30,31,36] and expanding it with respect to $\boldsymbol{k}$ up to the linear terms [30,31,37], Eq. (6) is rewritten as

$$\hat{g}^{\mathrm{r}}_{\boldsymbol{k},\omega} = [\hbar\omega + \epsilon_F - \hbar\tilde{v}_F \hat{\boldsymbol{\sigma}} \cdot (\boldsymbol{k} \times \boldsymbol{z}) + i\eta]^{-1}, \quad (7)$$

where $\tilde{v}_F = v_F/(1 + \xi)$ is the modified Fermi velocity due to nonmagnetic impurity scatterings with $\xi = n_i u_0^2/(4\pi\hbar^2 v_F^2)$ being a constant depending on the properties of the TI, and the imaginary part of the self-energy $\eta = \pi n_i u_0^2 \nu_e/2$ defines the transport relaxation time $\tau = \hbar/(2\eta)$. Here, $n_i = N_i/L^2$ is the concentration of the impurities on the surface and ν_e is the density of states of electrons on the surface. Since we are considering a metallic state, τ satisfies $\hbar/(\epsilon_F \tau) \ll 1$. By comparing Eqs. (2) and (7), we see that the effective Hamiltonian for the surface electrons affected by impurities is given by the right-hand side of Eq. (2) with replacing v_F with $\tilde{v}_F$. Accordingly, v_F in Eq. (4) is replaced by $\tilde{v}_F$. The detailed derivation is shown in Appendix A. Although the value of $\tilde{v}_F$ is almost the same as that of v_F [38], we keep $\tilde{v}_F$ instead of v_F in this paper so as to explicitly express the contribution from impurity scatterings.

III. SPIN AND CHARGE DENSITIES INDUCED BY AN APPLIED ELECTRIC FIELD

In this section, we calculate the response functions, i.e., the spin density and the charge density, to an applied electromagnetic field within the linear response theory. The results are summarized at the beginning of Sec. IV. Those who are interested only in the results can skip this section and go to Sec. IV.

We calculate the spin density induced by an applied electric field on a disordered surface of a doped TI by using the Keldysh Green's function method within the linear response to $\mathcal{H}_{\mathrm{em}}$. The spin density $\boldsymbol{s} = \frac{1}{2}\langle \psi^\dagger \hat{\boldsymbol{\sigma}} \psi \rangle$ is described by using the lesser component of the Keldysh-Green's function in the same position and time $-i\hbar\hat{G}^<(\boldsymbol{x},t,\boldsymbol{x},t) = \langle \psi^\dagger(\boldsymbol{x},t)\psi(\boldsymbol{x},t) \rangle$

as

$$s_i(\boldsymbol{x},t) = -\frac{i\hbar}{2}\mathrm{tr}[\hat{\sigma}_i \hat{G}^<(\boldsymbol{x},t,\boldsymbol{x},t)] \quad (i = x,y,z), \quad (8)$$

where tr denotes the trace over the spin indices. Then, from the Dyson's equation for $\hat{G}^<(\boldsymbol{x},t,\boldsymbol{x},t)$ the induced spin density within the linear response to $\mathcal{H}_{\mathrm{em}}$ is given by

$$s_\mu(\boldsymbol{x},t) = \frac{i\hbar e\tilde{v}_F}{2L^2} \sum_{v,u=x,y,z} \epsilon_{zvu} \sum_{\boldsymbol{q},\Omega} e^{i(\Omega t - \boldsymbol{q}\cdot\boldsymbol{x})}\mathrm{tr}[\hat{\Pi}_{\mu v}(\boldsymbol{q},\Omega)]$$
$$\times A_{\mathrm{em},u}(\boldsymbol{q},\Omega), \quad (9)$$

where ϵ_{zvu} is the Levi-Civita symbol, $\hat{\Pi}_{\mu v}$ is the spin-spin response function, and $\boldsymbol{q} = (q_x,q_y)$ and Ω are the momentum and frequency of $A_{\mathrm{em},u}(\boldsymbol{q},\Omega)$, respectively. The response function $\hat{\Pi}_{\mu v}$ can be decomposed as $\hat{\Pi}_{\mu v} = \hat{\sigma}_\mu \hat{\Pi}_v$ and $\hat{\Pi}_v$ is represented by

$$\hat{\Pi}_v(\boldsymbol{q},\Omega) = \sum_{\boldsymbol{k},\omega} \left[\hat{g}_{\boldsymbol{k}-\frac{q}{2},\omega-\frac{\Omega}{2}} \hat{\Lambda}_v(\omega,\boldsymbol{q},\Omega)\hat{g}_{\boldsymbol{k}+\frac{q}{2},\omega+\frac{\Omega}{2}}\right]^<. \quad (10)$$

Here, $\hat{\Lambda}_v$ is the vertex function due to $\mathcal{V}_{\mathrm{imp}}$, whose diagram is shown in Fig. 2, and is given by

$$\hat{\Lambda}_v(\omega,\boldsymbol{q},\Omega) = \hat{\sigma}_v + \sum_{\mu=0,x,y,z} \sum_{n=1}^\infty [\Gamma(\omega,\boldsymbol{q},\Omega)]^n_{v\mu}\hat{\sigma}_\mu, \quad (11)$$

where $\hat{\sigma}_0$ is the 2×2 identity matrix and Γ is a 4×4 matrix defined from the following equation:

$$\hat{\Gamma}_v(\omega,\boldsymbol{q},\Omega) \equiv n_i u_i^2 \sum_{\boldsymbol{k}} \hat{g}_{\boldsymbol{k}-\frac{q}{2},\omega-\frac{\Omega}{2}} \hat{\sigma}_v \hat{g}_{\boldsymbol{k}+\frac{q}{2},\omega+\frac{\Omega}{2}} \quad (12)$$

$$= \sum_{\mu=0,x,y,z} \Gamma_{v\mu}(\omega,\boldsymbol{q},\Omega)\hat{\sigma}_\mu. \quad (13)$$

Expanding Eq. (10) with respect to the retarded and advanced Green's functions, $\hat{g}^{\mathrm{r}}$ and $\hat{g}^{\mathrm{a}}$, based on the formula [33] $\hat{g}^<_{\boldsymbol{k},\omega} = f_\omega(\hat{g}^{\mathrm{a}}_{\boldsymbol{k},\omega} - \hat{g}^{\mathrm{r}}_{\boldsymbol{k},\omega})$, where $f_\omega \equiv 1/(e^{\beta\hbar\omega} + 1)$ is the Fermi distribution function, the spin-spin response function can be divided into three terms:

$$\hat{\Pi}_v(\boldsymbol{q},\Omega) = \hat{\Pi}^{\mathrm{ra}}_v(\boldsymbol{q},\Omega) + \hat{\Pi}^{\mathrm{rr}}_v(\boldsymbol{q},\Omega) + \hat{\Pi}^{\mathrm{aa}}_v(\boldsymbol{q},\Omega), \quad (14)$$

$$\hat{\Pi}^{\mathrm{ra}}_v(\boldsymbol{q},\Omega) \equiv \sum_{\boldsymbol{k},\omega} \left(f_{\omega+\frac{\Omega}{2}} - f_{\omega-\frac{\Omega}{2}}\right)\hat{g}^{\mathrm{r}}_{\boldsymbol{k}-\frac{q}{2},\omega-\frac{\Omega}{2}}$$
$$\times \hat{\Lambda}^{\mathrm{ra}}_v(\omega,\boldsymbol{q},\Omega)\hat{g}^{\mathrm{a}}_{\boldsymbol{k}+\frac{q}{2},\omega+\frac{\Omega}{2}}, \quad (15)$$

$$\hat{\Pi}^{\mathrm{rr}}_v(\boldsymbol{q},\Omega) \equiv -\sum_{\boldsymbol{k},\omega} f_{\omega+\frac{\Omega}{2}} \hat{g}^{\mathrm{r}}_{\boldsymbol{k}-\frac{q}{2},\omega-\frac{\Omega}{2}} \hat{\Lambda}^{\mathrm{rr}}_v(\omega,\boldsymbol{q},\Omega)\hat{g}^{\mathrm{r}}_{\boldsymbol{k}+\frac{q}{2},\omega+\frac{\Omega}{2}}, \quad (16)$$

$$\hat{\Pi}^{\mathrm{aa}}_v(\boldsymbol{q},\Omega) \equiv \sum_{\boldsymbol{k},\omega} f_{\omega-\frac{\Omega}{2}} \hat{g}^{\mathrm{a}}_{\boldsymbol{k}-\frac{q}{2},\omega-\frac{\Omega}{2}} \hat{\Lambda}^{\mathrm{aa}}_v(\omega,\boldsymbol{q},\Omega)\hat{g}^{\mathrm{a}}_{\boldsymbol{k}+\frac{q}{2},\omega+\frac{\Omega}{2}}. \quad (17)$$
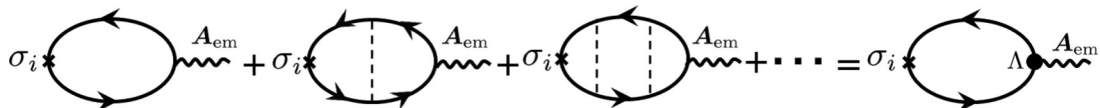

FIG. 2. Vertex function due to $\mathcal{V}_{\mathrm{imp}}$. The dashed and wavy lines mean the potential due to the nonmagnetic impurity scatterings and gauge coupling between conduction electrons and the electromagnetic field, respectively.

Here, $\hat{\Lambda}_\nu^{AB}$ (A,B = r,a) is defined by

$$\hat{\Lambda}_\nu^{AB}(\omega,\boldsymbol{q},\Omega) = \hat{\sigma}_\nu + \sum_{n=1}^{\infty}[\Gamma^{AB}(\omega,\boldsymbol{q},\Omega)]^n{}_{\nu\mu}\hat{\sigma}_\mu, \quad (18)$$

$$\hat{\Gamma}_\nu^{AB}(\omega,\boldsymbol{q},\Omega) \equiv n_i u_i^2 \sum_{\boldsymbol{k}} \hat{g}_{\boldsymbol{k}-\frac{q}{2},\omega-\frac{\Omega}{2}}^{A}\hat{\sigma}_\nu\hat{g}_{\boldsymbol{k}+\frac{q}{2},\omega+\frac{\Omega}{2}}^{B} \quad (19)$$

$$= \sum_{\mu=0,x,y,z}\Gamma_{\nu\mu}^{AB}(\omega,\boldsymbol{q},\Omega)\hat{\sigma}_\mu. \quad (20)$$

By expanding $\hat{\Gamma}_\nu^{rr}$ and $\hat{\Gamma}_\nu^{aa}$ with respect to $\boldsymbol{q}$ and Ω, we find that they are in the order of $\frac{\hbar}{\epsilon_F\tau} \ll 1$ and $\hat{\Lambda}_\nu^{rr}$ ($\hat{\Lambda}_\nu^{aa}$) in $\hat{\Pi}_\nu^{rr}$ ($\hat{\Pi}_\nu^{aa}$) can be approximated with $\hat{\sigma}_\nu$ (see Appendixes B–D for the detailed calculation). Then, by expanding the Fermi distribution function with respect to Ω, the dominant contributions of Eqs. (15), (16), and (17) are written by

$$\hat{\Pi}_\nu^{ra} = \Omega \sum_{\boldsymbol{k},\omega} f_\omega' \hat{g}_{\boldsymbol{k}-\frac{q}{2},\omega-\frac{\Omega}{2}}^{r}\hat{\Lambda}_\nu^{ra}(\omega,\boldsymbol{q},\Omega)\hat{g}_{\boldsymbol{k}+\frac{q}{2},\omega+\frac{\Omega}{2}}^{a}, \quad (21)$$

$$\hat{\Pi}_\nu^{rr} = -\sum_{\boldsymbol{k},\omega}\left\{ f_\omega \hat{g}_{\boldsymbol{k}-\frac{q}{2},\omega-\frac{\Omega}{2}}^{r}\hat{\sigma}_\nu\hat{g}_{\boldsymbol{k}+\frac{q}{2},\omega+\frac{\Omega}{2}}^{r} + \frac{1}{2}\Omega f_\omega' \hat{g}_{\boldsymbol{k}-\frac{q}{2},\omega-\frac{\Omega}{2}}^{r}\hat{\sigma}_\nu\hat{g}_{\boldsymbol{k}+\frac{q}{2},\omega+\frac{\Omega}{2}}^{r}\right\}, \quad (22)$$

$$\hat{\Pi}_\nu^{aa} = \sum_{\boldsymbol{k},\omega}\left\{ f_\omega \hat{g}_{\boldsymbol{k}-\frac{q}{2},\omega-\frac{\Omega}{2}}^{a}\hat{\sigma}_\nu\hat{g}_{\boldsymbol{k}+\frac{q}{2},\omega+\frac{\Omega}{2}}^{a} - \frac{1}{2}\Omega f_\omega' \hat{g}_{\boldsymbol{k}-\frac{q}{2},\omega-\frac{\Omega}{2}}^{a}\hat{\sigma}_\nu\hat{g}_{\boldsymbol{k}+\frac{q}{2},\omega+\frac{\Omega}{2}}^{a}\right\}. \quad (23)$$

In addition, $\hat{\Pi}_\nu^{rr}$ and $\hat{\Pi}_\nu^{aa}$ are shown to be much smaller than $\hat{\Pi}_\nu^{ra}$ (the detailed calculation is given in Appendix E). Thus, $\hat{\Pi}_\nu$ is approximately given by

$$\hat{\Pi}_\nu \simeq \hat{\Pi}_\nu^{ra} = \Omega \sum_{\boldsymbol{k},\omega} f_\omega' \hat{g}_{\boldsymbol{k}-\frac{q}{2},\omega-\frac{\Omega}{2}}^{r}\hat{\Lambda}_\nu^{ra}(\omega,\boldsymbol{q},\Omega)\hat{g}_{\boldsymbol{k}+\frac{q}{2},\omega+\frac{\Omega}{2}}^{a}. \quad (24)$$

In the low-temperature limit, we approximate the derivative of the Fermi distribution function as $f_\omega' = -\delta(\omega)$. Then, the integral over ω in $\hat{\Pi}_\nu^{ra}$ reduces to

$$\hat{\Pi}_\nu^{ra}(\boldsymbol{q},\Omega) = -\frac{\Omega}{2\pi}\sum_{\boldsymbol{k}}\hat{g}_{\boldsymbol{k}-\frac{q}{2},-\frac{\Omega}{2}}^{r}\hat{\Lambda}_\nu^{ra}(0,\boldsymbol{q},\Omega)\hat{g}_{\boldsymbol{k}+\frac{q}{2},\frac{\Omega}{2}}^{a}. \quad (25)$$

We further expand $\hat{\Lambda}_\nu^{ra}$ as $\hat{\Lambda}_\nu^{ra} = \sum_{\alpha=0,x,y,z}\hat{\sigma}_\alpha\Lambda_{\nu\alpha}^{ra}$, and rewrite Eq. (25) as

$$\hat{\Pi}_\nu^{ra}(\boldsymbol{q},\Omega) = -\frac{\Omega}{2\pi}\sum_{\zeta=0,x,y,z}\hat{I}_\zeta(\boldsymbol{q},\Omega)\Lambda_{\nu\zeta}^{ra}(0,\boldsymbol{q},\Omega). \quad (26)$$

Here, we define $\hat{I}_\zeta(\boldsymbol{q},\Omega) \equiv \sum_{\boldsymbol{k}}\hat{g}_{\boldsymbol{k}-\frac{q}{2},-\frac{\Omega}{2}}^{r}\hat{\sigma}_\zeta\hat{g}_{\boldsymbol{k}+\frac{q}{2},\frac{\Omega}{2}}^{a}$, which is calculated up to the quadratic terms in q and the primary terms in Ω as (see Appendixes B and C for the detailed derivation)

$$\hat{I}_{\zeta=0} = \frac{\pi\nu_e}{2\eta}\left[\left(1 - i\Omega\tau - \frac{1}{2}\ell^2 q^2\right)\hat{\sigma}_0 + \sum_{\alpha,u=x,y}\frac{i}{2}\ell\hat{\sigma}_u q_\alpha \epsilon_{u\alpha z}\right] + O\left(\frac{\hbar}{\epsilon_F\tau}\right), \quad (27)$$

$$\hat{I}_{\zeta=x,y} = \frac{\pi\nu_e}{2\eta}\left[\sum_{\nu=x,y}\left\{\frac{1}{2}\left(1 - i\Omega\tau - \frac{3}{4}\ell^2 q^2\right)\delta_{\zeta\nu} + \frac{1}{4}\ell^2 q_\zeta q_\nu\right\}\hat{\sigma}_\nu + \sum_{\alpha=x,y}\frac{i}{2}\ell\hat{\sigma}_0 q_\alpha \epsilon_{\zeta\alpha z}\right] + O\left(\frac{\hbar}{\epsilon_F\tau}\right), \quad (28)$$

$$\hat{I}_{\zeta=z} = O\left(\frac{\hbar}{\epsilon_F\tau}\right), \quad (29)$$

where $\ell = \tilde{v}_F\tau$ is the mean-free path. Since $\hat{I}_{\zeta=z}$ is negligibly small as compared with $\hat{I}_{\zeta=0}$ and $\hat{I}_{\zeta=x,y}$, we consider only the contributions from $\hat{I}_{\zeta=0,x,y}$. Since Eqs. (27) and (28) do not include $\hat{\sigma}_z$, they are represented by using the Pauli matrices as

$$\hat{I}_\zeta = \sum_{\mu=0,x,y}I_{\zeta\mu}\hat{\sigma}_\mu + O\left(\frac{\hbar}{\epsilon_F\tau}\right), \quad (30)$$

where $I_{\zeta\mu}$ is the 3×3 symmetric matrix given by

$$I = \frac{\pi\nu_e}{2\eta}\begin{pmatrix} 1 - i\Omega\tau - \frac{1}{2}\ell^2 q^2 & \frac{i}{2}\ell q_y & -\frac{i}{2}\ell q_x \\ \frac{i}{2}\ell q_y & \frac{1}{2}\left(1 - i\Omega\tau - \frac{1}{2}\ell^2 q^2\right) + \frac{1}{8}\ell^2\left(q_x^2 - q_y^2\right) & \frac{1}{4}\ell^2 q_x q_y \\ -\frac{i}{2}\ell q_x & \frac{1}{4}\ell^2 q_x q_y & \frac{1}{2}\left(1 - i\Omega\tau - \frac{1}{2}\ell^2 q^2\right) - \frac{1}{8}\ell^2\left(q_x^2 - q_y^2\right) \end{pmatrix}. \quad (31)$$

On the other hand, from Eq. (18), the vertex function $\hat{\Lambda}_\nu^{ra}$ can be described by

$$\hat{\Lambda}_\nu^{ra} = \hat{\sigma}_\nu + \sum_{\alpha=0,x,y}\Gamma_{\nu\alpha}^{ra}\hat{\sigma}_\alpha + \sum_{\alpha=0,x,y}[(\Gamma^{ra})^2]_{\nu\alpha}\hat{\sigma}_\alpha + \cdots = \sum_{\alpha=0,x,y}[(1 - \Gamma^{ra})^{-1}]_{\nu\alpha}\hat{\sigma}_\alpha, \quad (32)$$

where the second equality holds when $\max\{\sum_\nu |\Gamma^{\mathrm{ra}}_{\mu\nu}|\} < 1$ is satisfied. By using $1 - i\Omega\tau = \frac{1}{1+i\Omega\tau} + O(\Omega^2)$, $\Gamma^{\mathrm{ra}} = n_i u_i^2 I$, and Eq. (31), one can see Γ^{ra} indeed satisfies $\max\{\sum_\nu |\Gamma^{\mathrm{ra}}_{\mu\nu}|\} < 1$. Then, the matrix $\Gamma^{\mathrm{ra}}\Lambda^{\mathrm{ra}}$ is calculated as

$$\Gamma^{\mathrm{ra}}\Lambda^{\mathrm{ra}} = -1 + (1 - \Gamma^{\mathrm{ra}})^{-1} = \begin{pmatrix} 0 & 0 & 0 \\ 0 & 1 & 0 \\ 0 & 0 & 1 \end{pmatrix} + \begin{pmatrix} \frac{1}{q^2\ell^2 + i\Omega\tau} & \frac{i\ell q_y}{q^2\ell^2 + i\Omega\tau} & -\frac{i\ell q_x}{q^2\ell^2 + i\Omega\tau} \\ \frac{i\ell q_y}{q^2\ell^2 + i\Omega\tau} & -\frac{q_y^2\ell^2}{q^2\ell^2 + i\Omega\tau} & \frac{q_x q_y\ell^2}{q^2\ell^2 + i\Omega\tau} \\ -\frac{i\ell q_x}{q^2\ell^2 + i\Omega\tau} & \frac{q_x q_y\ell^2}{q^2\ell^2 + i\Omega\tau} & -\frac{q_x^2\ell^2}{q^2\ell^2 + i\Omega\tau} \end{pmatrix}, \tag{33}$$

from which we obtain the spin-spin response function as

$$\hat{\Pi}_\nu \simeq -\frac{\Omega\nu_e}{4\eta} \sum_{\zeta'=0,x,y} [\Gamma^{\mathrm{ra}}\Lambda^{\mathrm{ra}}]_{\zeta'\nu}\hat{\sigma}_{\zeta'}, \tag{34}$$

where we have used the fact that I and Λ^{ra} are symmetric matrices. Thus, from Eqs. (9) and (34), the $\mu = x, y$ components of the spin density are given by

$$s_\mu = -\frac{e\tilde{v}_{\mathrm{F}}\nu_e\tau}{2L^2}\epsilon_{zvu}\partial_t \sum_{\boldsymbol{q},\Omega} e^{i(\Omega t - \boldsymbol{q}\cdot\boldsymbol{x})}[\Gamma^{\mathrm{ra}}\Lambda^{\mathrm{ra}}]_{\mu\nu}A_{\mathrm{em},u}. \tag{35}$$

Substituting Eq. (33) in (35), we obtain

$$s_x = \frac{1}{2}e\tilde{v}_{\mathrm{F}}\nu_e\tau E_y + \frac{e\tilde{v}_{\mathrm{F}}\nu_e\tau}{2L^2}\partial_t \sum_{\boldsymbol{q},\Omega} e^{i(\Omega t - \boldsymbol{q}\cdot\boldsymbol{x})}\frac{\ell^2\left(q_y^2 A_{\mathrm{em},y} + q_y q_x A_{\mathrm{em},x}\right)}{q^2\ell^2 + i\Omega\tau}, \tag{36}$$

$$s_y = -\frac{1}{2}e\tilde{v}_{\mathrm{F}}\nu_e\tau E_x - \frac{e\tilde{v}_{\mathrm{F}}\nu_e\tau}{2L^2}\partial_t \sum_{\boldsymbol{q},\Omega} e^{i(\Omega t - \boldsymbol{q}\cdot\boldsymbol{x})}\frac{\ell^2\left(q_x^2 A_{\mathrm{em},x} + q_y q_x A_{\mathrm{em},y}\right)}{q^2\ell^2 + i\Omega\tau}. \tag{37}$$

The second terms of Eqs. (36) and (37) can be described by using the charge density ρ_e on the surface. Here, $\rho_e \equiv e\langle\psi^\dagger\psi\rangle = \frac{i\hbar e^2 \tilde{v}_{\mathrm{F}}}{L^2}\epsilon_{zvu}\sum_{\boldsymbol{q},\Omega} e^{i(\Omega t - \boldsymbol{q}\cdot\boldsymbol{x})}\mathrm{tr}[\hat{\Pi}^{\mathrm{ra}}_{0\nu}]A_{\mathrm{em},u}(\boldsymbol{q},\Omega)$ is obtained from the charge-spin response function $\hat{\Pi}_{0\nu} = \hat{\Pi}_\nu$ as

$$\rho_e = -\frac{i\hbar e^2 \tilde{v}_{\mathrm{F}}\nu_e}{2\eta L^2}\epsilon_{zvu}\sum_{\boldsymbol{q},\Omega} e^{i(\Omega t - \boldsymbol{q}\cdot\boldsymbol{x})}\Omega\{[\Gamma^{\mathrm{ra}}\Lambda^{\mathrm{ra}}]_{0\nu}A_{\mathrm{em},u}\} = \frac{e^2\tilde{v}_{\mathrm{F}}\nu_e\tau}{L^2}\ell\partial_t\nabla_\nu \sum_{\boldsymbol{q},\Omega} e^{i(\Omega t - \boldsymbol{q}\cdot\boldsymbol{x})}\frac{1}{q^2\ell^2 + i\Omega\tau}A_{\mathrm{em},v} \tag{38}$$

$$= -2e^2\nu_e D\tau \nabla\cdot\langle\boldsymbol{E}\rangle_{\mathrm{D}}, \tag{39}$$

where $D \equiv \frac{1}{2}\tilde{v}_{\mathrm{F}}^2\tau = \frac{1}{2}\tilde{v}_{\mathrm{F}}\ell$ is the diffusion constant. Here, $\langle\boldsymbol{E}\rangle_{\mathrm{D}}$ is defined by the convolution of $\boldsymbol{E}$ and the diffusive propagation function $\mathcal{D}$ as

$$\langle\boldsymbol{E}\rangle_{\mathrm{D}} \equiv \frac{1}{\tau}\int_{-\infty}^{\infty} dt' \int d\boldsymbol{x}'\mathcal{D}(\boldsymbol{x} - \boldsymbol{x}', t - t')\boldsymbol{E}(\boldsymbol{x}', t'), \quad (40)$$

$$\mathcal{D}(\boldsymbol{x}, t) = \frac{1}{L^2}\sum_{\boldsymbol{q},\Omega} e^{i(\Omega t - \boldsymbol{q}\cdot\boldsymbol{x})}\frac{1}{2Dq^2 + i\Omega} \tag{41}$$

$$\sim \frac{\theta(t)}{8\pi Dt}\exp\left[-\frac{|\boldsymbol{x}|^2}{8Dt}\right]. \tag{42}$$

The diffusive propagation function $\mathcal{D}$ is also the Green's function satisfying the following differential equation:

$$(\partial_t - 2D\nabla^2)\mathcal{D}(\boldsymbol{x}, t) = \delta(\boldsymbol{x})\delta(t). \tag{43}$$

Equations (39) and (40) show that due to the impurities, the effect of the applied electric field on the surface electrons is not instantaneous but diffusively propagates on the surface of the TI. Equation (40) gives the definition of such a nonlocal electric field. Suppose that the surface of the TI is isotropic, the gradient of the charge density is given by

$$\nabla_x \rho_e = -\frac{e^2\tilde{v}_{\mathrm{F}}\nu_e\tau}{L^2}\partial_t \sum_{\boldsymbol{q},\Omega} e^{i(\Omega t - \boldsymbol{q}\cdot\boldsymbol{x})}\frac{\ell\left(q_x^2 A_{\mathrm{em},x} + q_y q_x A_{\mathrm{em},y}\right)}{q^2\ell^2 + i\Omega\tau}, \tag{44}$$

$$\nabla_y \rho_e = -\frac{e^2\tilde{v}_{\mathrm{F}}\nu_e\tau}{L^2}\partial_t \sum_{\boldsymbol{q},\Omega} e^{i(\Omega t - \boldsymbol{q}\cdot\boldsymbol{x})}\frac{\ell\left(q_y^2 A_{\mathrm{em},y} + q_y q_x A_{\mathrm{em},x}\right)}{q^2\ell^2 + i\Omega\tau}, \tag{45}$$

which is related to the spin density [Eqs. (36) and (37)] as

$$\boldsymbol{s} = \frac{1}{2}e\tilde{v}_{\mathrm{F}}\nu_e\tau(\boldsymbol{E}\times\boldsymbol{z}) + \frac{\ell}{2e}(\boldsymbol{z}\times\nabla)\rho_e. \tag{46}$$

On the other hand, the spin density on the surface of the TI is related to the charge current via

$$j_\mu = -\frac{\partial\mathcal{H}_{\mathrm{em}}}{\partial A_{\mathrm{em},\mu}} = 2e\tilde{v}_{\mathrm{F}}(\boldsymbol{z}\times\boldsymbol{s})_\mu, \tag{47}$$

where we have replaced v_{F} in Eq. (4) with $\tilde{v}_{\mathrm{F}}$ so as to take into account the effects of impurities. By substituting Eq. (46) in (47), we obtain

$$\boldsymbol{j} = e^2\tilde{v}_{\mathrm{F}}^2\nu_e\tau\boldsymbol{E} - \tilde{v}_{\mathrm{F}}\ell\nabla\rho_e. \tag{48}$$

We have confirmed that Eqs. (39) and (48) satisfy the charge conservation law $\dot{\rho}_e + \nabla\cdot\boldsymbol{j} = 0$ (see Appendix G for the detailed calculation).

TABLE I. Dependence on the applied electric field $\boldsymbol{E}$ of the induced charge density ρ_e, spin current density j_i^α, spin density $\boldsymbol{s}$, and charge current density $\boldsymbol{j}$ on a disordered surface of a doped TI, where $\langle \boldsymbol{E} \rangle_{\mathrm{D}}$ is defined in Eq. (40).

	ρ_e (Charge density)	j_i^α (Spin current)	$\boldsymbol{s}$ (Spin density)	$\boldsymbol{j}$ (Charge current)
Local			$\boldsymbol{z} \times \boldsymbol{E}$	$\boldsymbol{E}$
Nonlocal	$\boldsymbol{\nabla} \cdot \langle \boldsymbol{E} \rangle_{\mathrm{D}}$	$\epsilon_{z\alpha i} \boldsymbol{\nabla} \cdot \langle \boldsymbol{E} \rangle_{\mathrm{D}}$	$(\boldsymbol{z} \times \boldsymbol{\nabla}) \boldsymbol{\nabla} \cdot \langle \boldsymbol{E} \rangle_{\mathrm{D}}$	$\boldsymbol{\nabla}(\boldsymbol{\nabla} \cdot \langle \boldsymbol{E} \rangle_{\mathrm{D}})$

IV. PROPERTIES OF THE CHARGE, SPIN, CHARGE CURRENT, AND SPIN CURRENT DENSITIES

We summarize the results obtained in the previous section [Eqs. (39), (46), and (48)] in Table I. Using the above results, we discuss the property of the charge, spin, charge current, and spin current densities induced by an electric field applied on the disordered surface of the doped TI. We find that there are two types of quantities induced by the applied electric field: one is directly proportional to the electric field $\boldsymbol{E}$, such as the first terms of Eqs. (46) and (48), and the other relates to $\boldsymbol{E}$ via $\langle \boldsymbol{E} \rangle_{\mathrm{D}}$, such as the second terms of Eqs. (46) and (48). We define the former (latter) as the local (nonlocal) quantity and decompose Eqs. (46) and (48) as

$$\boldsymbol{j} = \boldsymbol{j}^{(\mathrm{l})} + \boldsymbol{j}^{(\mathrm{nl})}, \tag{49}$$

$$\boldsymbol{s} = \boldsymbol{s}^{(\mathrm{l})} + \boldsymbol{s}^{(\mathrm{nl})}, \tag{50}$$

where $\boldsymbol{j}^{(\mathrm{l})}$ ($\boldsymbol{s}^{(\mathrm{l})}$) and $\boldsymbol{j}^{(\mathrm{nl})}$ ($\boldsymbol{s}^{(\mathrm{nl})}$) are local and nonlocal charge current (spin) density, respectively. In the following sections, first, we show the properties of the local quantities (Sec. IV A). Next, we consider the physical meaning of the charge density (Sec. IV B), and show the nonlocal charge current and spin density (Sec. IV C), which are proportional to the spatial gradient of the charge density, as shown in Table I. Finally, we discuss the property of the spin current (Sec. IV D).

A. Local charge current and spin density

From Eq. (48), the local part of the charge current is given by

$$\boldsymbol{j}^{(\mathrm{l})}(\boldsymbol{x},t) = e^2 \tilde{v}_{\mathrm{F}}^2 \nu_e \tau \boldsymbol{E}(\boldsymbol{x},t). \tag{51}$$

The local charge current is directly induced by the applied electric field $\boldsymbol{E}(\boldsymbol{x},t)$: as in the conventional metal, electric current emerges in the direction of the applied electric field. The conductivity $\boldsymbol{j}^{(\mathrm{l})}/\boldsymbol{E}$ is proportional to $\tilde{v}_{\mathrm{F}}^2$ and τ. These properties are consistent with the previous works [8,32].

Due to the spin-momentum locking, the spin density is also induced by the electric field [7–9,32], which corresponds to the local spin density given by the first term of Eq. (46):

$$\boldsymbol{s}^{(\mathrm{l})} = \frac{1}{2} e \tilde{v}_{\mathrm{F}} \nu_e \tau (\boldsymbol{E} \times \boldsymbol{z}). \tag{52}$$

It is found that the induced spin density is perpendicular to the applied electric field. The magnitude of the local spin density depends on the relaxation time. These properties agree with the existing works [7–9,32]. The phenomenon of the electric field induced spin polarization is similar to the Edelstein effect [39], which occurs in the presence of the Rashba-type spin-orbit interaction in a two-dimensional system.

B. Charge density

We find that as shown in Eq. (39) the charge density ρ_e is induced by the divergence of the electric field with diffusion: $\boldsymbol{\nabla} \cdot \langle \boldsymbol{E} \rangle_{\mathrm{D}}$. Therefore, when we apply a uniform electric field, no charge density is induced. From Eqs. (40)–(42) we obtain the diffusion equation for the charge transport:

$$(\partial_t - 2D\nabla^2)\rho_e(\boldsymbol{x},t) = -2e^2\nu_e D\boldsymbol{\nabla} \cdot \boldsymbol{E}(\boldsymbol{x},t), \tag{53}$$

which indicates that the divergence of the applied electric field works as a source of the diffusive propagation of the charge density. We find that from the left side of the equation above, $(\partial_t - 2D\nabla^2)\rho_e$, the diffusion constant is $2D$, twice of that on the surface of a metal [31]. The factor 2 comes from the difference in the self-energy due to impurity scattering: The self-energy on the surface of an isotropic metal is given by $\pi n_\mathrm{i} u_\mathrm{i}^2 \nu_{e,m}$, where $\nu_{e,m}$ is the density of states in the metal, whereas that on the surface of the TI is $\frac{1}{2}\pi n_\mathrm{i} u_\mathrm{i}^2 \nu_e$. The factor $\frac{1}{2}$, which originates from the linear dispersion of the surface of the TI, leads to the coefficient $2D$. Here, the diffusive equation of motion qualitatively agrees with the previous works [32,40,41].

C. Nonlocal charge current and spin density

Next, we consider the nonlocal charge current and spin density. The nonlocal charge current density corresponds to the second term of Eq. (48):

$$\boldsymbol{j}^{(\mathrm{nl})} = e^2 \tilde{v}_{\mathrm{F}}^2 \ell^2 \nu_e \tau \boldsymbol{\nabla}(\boldsymbol{\nabla} \cdot \langle \boldsymbol{E} \rangle_{\mathrm{D}}). \tag{54}$$

It is found that the nonlocal charge current is proportional to the spatial gradient of the charge density, which is shown in the previous subsection as $\boldsymbol{j}^{(\mathrm{nl})} = -\tilde{v}_{\mathrm{F}}\ell\boldsymbol{\nabla}\rho_e$. The charge current in this form indicates that the nonlocal charge current is a diffusion current induced by the inhomogeneous charge density. Since both the local and nonlocal charge currents are proportional to $\tilde{v}_{\mathrm{F}}^2$, their directions are the same for top and bottom surfaces of the TI.

Due to the spin-momentum locking, the nonlocal spin density $\boldsymbol{s}^{(\mathrm{nl})} = \frac{\ell}{2e}(\boldsymbol{z} \times \boldsymbol{\nabla})\rho_e$, which corresponds to the second term of Eq. (46), is induced on the surface. The nonlocal spin is given by

$$\boldsymbol{s}^{(\mathrm{nl})} = -\frac{e\tilde{v}_{\mathrm{F}}\nu_e\tau\ell^2}{2}(\boldsymbol{z} \times \boldsymbol{\nabla})(\boldsymbol{\nabla} \cdot \langle \boldsymbol{E} \rangle_{\mathrm{D}}). \tag{55}$$

The spin density is generated by the second spatial derivative of the nonlocal electric field $\langle \boldsymbol{E} \rangle_{\mathrm{D}}$.

The nonlocal spin density diffusively propagates through the impurity scatterings on the surface of the TI. The diffusion propagation of the spin is described by

$$(\partial_t - 2D\nabla^2)\boldsymbol{s}^{(\mathrm{nl})} = -\frac{e\tilde{v}_{\mathrm{F}}\nu_e\ell^2}{2}(\boldsymbol{z} \times \boldsymbol{\nabla})(\boldsymbol{\nabla} \cdot \boldsymbol{E}). \tag{56}$$

We find that the diffusion propagation of the spin is triggered by an inhomogeneous electric field $\nabla(\nabla \cdot \boldsymbol{E})$. (This property is also predicted in Ref. [34].) Hence, when we apply a uniform electric field on the surface, the nonlocal spin density is not generated. As in the case of charge density, the diffusion constant for the spin density is $2D$.

We note that both the local and nonlocal spin densities are proportional to $\tilde{v}_F$. Since $\tilde{v}_F$'s on the top and the bottom sides of the TI have opposite signs, the direction of the induced spin on the top surface of the TI is perfectly opposite to that on the bottom surface of the TI, when we apply the same electric field on both the top and bottom sides of the TI.

D. Spin current

Next, we calculate the spin current due to the applied electric field on the disordered surface of the doped TI. The spin current j_i^α is defined by

$$\dot{s}^\alpha + \nabla_i j_i^\alpha = \mathcal{T}^\alpha, \tag{57}$$

where the subscript and superscript of j_i^α denote the direction of the flow and spin, respectively, and $\mathcal{T}^\alpha$ represents the spin relaxation. Using the Hamiltonian in Eq. (3) and the Heisenberg equation for s^α, we obtain

$$j_i^\alpha = \frac{\tilde{v}_F}{2e} \epsilon_{z\alpha i} \rho_e. \tag{58}$$

The index z denotes the out-of-plane direction and $\epsilon_{z\alpha i}$ means that the direction of the spin and that of the spin current are both in the xy plane and perpendicular to each other. Note that the direction of the flow and spin is perpendicular to each other. This is the consequence of the spin-momentum locking on the surface of the TI. We also note that the spin current is proportional to the charge density, and from Eq. (39), proportional to the divergence of the nonlocal electric field:

$$j_i^\alpha = -e\tilde{v}_F \nu_e D\tau \epsilon_{z\alpha i} \nabla \cdot \langle \boldsymbol{E} \rangle_D. \tag{59}$$

Hence, when we apply a spatially uniform electric field on the surface, no spin current is induced. Besides, we find that the spin current is an odd function of $\tilde{v}_F$, which means the spin current depends on the chirality on the surface of the TI. Namely, the relative direction between flow and spin of j_i^α on the top side of the TI is opposite to that on the bottom side of the TI.

In the conventional spin-orbit coupled systems, the spin current is generated by an applied electric field [42–46], which is called the spin Hall effect. Besides, the generated spin current can be converted into the charge current via the spin-orbit interaction [47]. These effects can be understood from the coupling between the spin current and the charge current: $j_i \propto \epsilon_{ij\alpha} j_j^\alpha$ [47]. On the surface of the TI, on the other hand, we find from Eqs. (54) and (59) that the nonlocal charge current is proportional to the gradient of the spin current [37]:

$$\boldsymbol{j}^{(\mathrm{nl})} = -e\ell \epsilon_{z\alpha i} \nabla j_i^\alpha. \tag{60}$$

Again, this is the consequence of the spin-momentum locking and Eq. (60) generally holds for the system of electrons on a surface of TIs [37]. This property in the TI is distinct from that in a conventional metal. The direction of the charge current is parallel to the spatial gradient of j_i^α. This relation is plausible due to the following reasons. First, the charge density ρ_e is proportional to the spin current. Second, a diffusive particle current is generally proportional to a spatial gradient of particles. We note that there is no relation between the spin current and the local charge current $\boldsymbol{j}^{(1)}$.

Finally, we comment on the property of the spin relaxation torque. The relaxation torque $\mathcal{T}^\alpha$ defined in Eq. (57) is obtained within the linear response to the electric field as

$$
\begin{aligned}
\mathcal{T}^\alpha &= \frac{1}{2} e\tilde{v}_F \nu_e \tau (\dot{\boldsymbol{E}} \times z)_\alpha - \left(\frac{\ell}{2e}\partial_t + \frac{\tilde{v}_F}{2e}\right)(z \times \nabla)_\alpha \rho_e \\
&= \frac{1}{2} e\tilde{v}_F \nu_e [\tau(\dot{\boldsymbol{E}} \times z)_\alpha + 2D\tau(z \times \nabla)_\alpha (\nabla \cdot \langle \boldsymbol{E}\rangle_D)] \\
&\quad + o[(z \times \nabla)_\alpha (\nabla \cdot \langle \dot{\boldsymbol{E}}\rangle_D)]. \tag{61}
\end{aligned}
$$

Here, $\mathcal{T}^\alpha$ can be divided into the local and nonlocal terms, which correspond to the first and second terms, respectively, in the first square brackets in the most right-hand side of Eq. (61). The local one is given by the time derivative of the applied electric field, and its direction is perpendicular to both $\dot{\boldsymbol{E}}$ and z. The nonlocal one is proportional to the second derivative of the nonlocal electric field $\langle \boldsymbol{E}\rangle_D$. These above results and properties are the same as the spin density on the surface of the TI with magnetism [37].

V. RESPONSES TO THE ELECTRIC FIELD OF A TWISTED LIGHT BEAM

Using the results obtained in Sec. IV, we discuss the properties of the spin and charge densities due to the electric field of a twisted light beam with various orbital angular momenta.

A. Electric field of a twisted light beam

First, we explain the property of the electric field of the twisted light beam with the Laguerre-Gaussian modes [24,26]. We assume that the twisted light beam propagates along the z axis and the electric field of the twisted light beam lies in the xy plane at the top surface of the TI ($z = z_0$). The schematic of the system is illustrated in Fig. 3. The twisted light beam satisfies the wave equation $\nabla^2 \boldsymbol{E} - \frac{1}{c_0^2}\frac{\partial^2 \boldsymbol{E}}{\partial t^2} = 0$, where
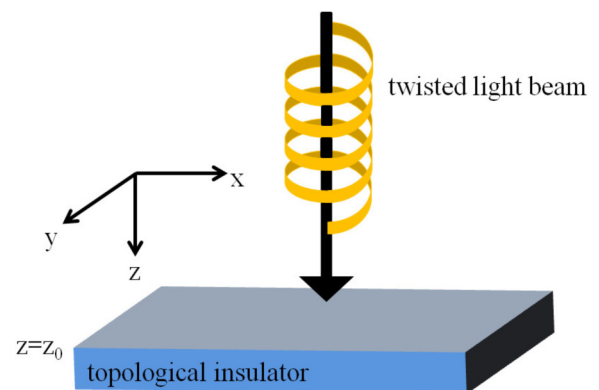

FIG. 3. Schematic illustration of the system. The optical twisted light beam is applied to the surface of the topological insulator for normal incidence.

c_0 is the velocity of light in a vacuum. Then, the electric field $\boldsymbol{E}(\boldsymbol{x},t) = (E_x(r,\varphi,t), E_y(r,\varphi,t))$ on the surface is written by [24,26]

$$
\begin{aligned}
\boldsymbol{E} = \mathcal{E} \big(&\cos\left(\Theta_{\mathcal{R}} + m_{\mathrm{L}}^z \varphi - \Omega t\right), \\
&- \sigma_{\mathrm{L}}^z \sin\left(\Theta_{\mathcal{R}} + m_{\mathrm{L}}^z \varphi - \Omega t\right) \big),
\end{aligned}
\tag{62}
$$

where $r = \sqrt{x^2 + y^2}$ is the distance from the center of the light on the top surface ($z = z_0$) and $\varphi = \arctan(y/x)$ is the azimuthal angle. The helicity $\sigma_{\mathrm{L}}^z = +1(-1)$ denotes the right-hand (left-hand) circularly polarized light and corresponds to the spin angular momentum of light $+1$ (-1). The orbital angular momentum of light $m_{\mathrm{L}}^z = 0, \pm 1, \dots$ determines the whirling pattern of the electric field on the plane at $z = z_0$, which can be manipulated in experiments [26]. The phase $\Theta_{\mathcal{R}} \equiv \Theta_{\mathcal{R}}(r,z_0)$ depends on r and the distance from the light source z and is given by [28]

$$
\Theta_{\mathcal{R}} = -\left(1 + 2p + |m_{\mathrm{L}}^z|\right) \tan^{-1}\left[\frac{z_0}{z_r}\right] - \frac{q_z r^2}{2R(z_0)},
\tag{63}
$$

where the first term denotes Guoy phase, $R(z) \equiv z[1 + (z_r/z)^2]$ is the radius of the beam curvature with taking of the z axis at the beam waist, $z_r = \pi d_0^2 / \lambda$ is the Rayleigh range, d_0 is the waist size of the $m_{\mathrm{L}}^z = p = 0$ mode, λ is the wavelength, and q_z is the wave vector of the light. The integer p is one of the indices that specifies the Laguerre-Gaussian mode and denotes the number of oscillations of the electric field $\mathcal{E}$ in the radial direction. Here, $\mathcal{E}$ is given by

$$
\begin{aligned}
\mathcal{E}(r,z_0) = \mathcal{E}_0 &\sqrt{\frac{2p!}{\pi\left(p + |m_{\mathrm{L}}^z|\right)! [1 + (z_0/z_r)^2]}} \\
&\times (\sqrt{2}u)^{|m_{\mathrm{L}}^z|} L_{|m_{\mathrm{L}}^z|}^p (2u^2) \exp(-u^2),
\end{aligned}
\tag{64}
$$

where $u = r/\{d_0[1 + (z_0/z_r)^2]^{\frac{1}{2}}\}$, $\mathcal{E}_0$ is a constant, and $L_{|m_{\mathrm{L}}^z|}^p(y)$ is the Laguerre polynomial defined by

$$
L_{|m_{\mathrm{L}}^z|}^p(y) = \sum_{k=0}^{p} (-1)^k \frac{\left(|m_{\mathrm{L}}^z| + p\right)!}{(p-k)!\left(k + |m_{\mathrm{L}}^z|\right)! k!} y^k.
\tag{65}
$$

In the following discussion, we consider only the $p = 0$ modes. We also assume that the twisted light beam is focused at the surface of the TI, i.e., $z_0 = 0$. Then, the phase $\Theta_{\mathcal{R}}$ becomes zero, and the magnitude $\mathcal{E}$ defined in Eq. (64) reduces to

$$
\mathcal{E}(r,0) = \mathcal{E}_0 \sqrt{\frac{2}{\pi |m_{\mathrm{L}}^z|!}} \left(\frac{\sqrt{2}r}{d_0}\right)^{|m_{\mathrm{L}}^z|} \exp\left(-\frac{r^2}{d_0^2}\right).
\tag{66}
$$

Figures 4(a)–4(d) show the snapshots of the electric field for $\sigma_{\mathrm{L}}^z = -1$ and $m_{\mathrm{L}}^z = 0, 1, 2$, and -1. In both cases of $m_{\mathrm{L}}^z = 0$ and $m_{\mathrm{L}}^z \neq 0$, the amplitude of the electric field exponentially decays with r^2. In addition to this, for the cases of nonzero m_{L}^z, the magnitude of the electric field vanishes at $r = 0$ because of the phase singularity. This is a characteristic property of the twisted light beam. Besides, the direction of the electric field depends on the polar angle around the center of the incident light: While the direction of the electric field is uniform for $(\sigma_{\mathrm{L}}^z, m_{\mathrm{L}}^z) = (-1,0)$ [Fig. 4(a)], the direction of the electric field at $(\sigma_{\mathrm{L}}^z, m_{\mathrm{L}}^z) = (-1,1)$ rotates by 2π in the counterclockwise direction as one goes around the beam center from $\varphi = 0$ to
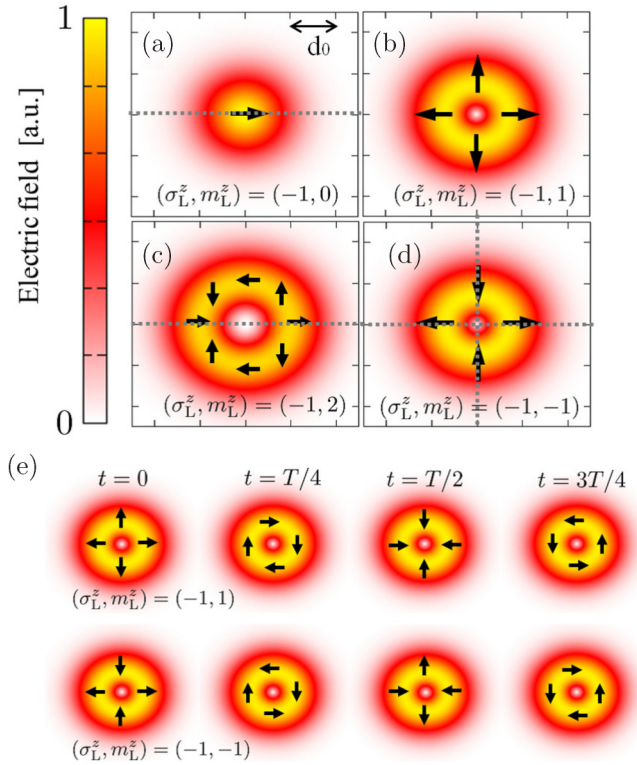

FIG. 4. (a)–(d) Snapshots of the electric field induced by the twisted light beam with (a) $(\sigma_{\mathrm{L}}^z, m_{\mathrm{L}}^z) = (-1,0)$, (b) $(-1,1)$, (c) $(-1,2)$, and (d) $(-1,-1)$, where σ_{L}^z and m_{L}^z denote the spin and orbital angular momentum of light, respectively. Shown are density plots of the magnitude of the electric field, and the black arrows show the direction of the electric field. d_0 is the waist size for the $m_{\mathrm{L}}^z = 0$ mode. (e) Time evolution of the electric field with $(\sigma_{\mathrm{L}}^z, m_{\mathrm{L}}^z) = (-1,1)$ (top) and $(-1,-1)$ (bottom), where $T = 2\pi/\Omega$ with Ω being the angular frequency of the light.

2π [Fig. 4(b)]. Similarly for the cases of $(\sigma_{\mathrm{L}}^z, m_{\mathrm{L}}^z) = (-1,2)$ and $(-1,-1)$, the direction of the electric field changes by 4π and -2π, respectively [Figs. 4(c) and 4(d)]. Note that the configurations shown in Figs. 4(a)–4(d) are snapshots and they evolve in time depending on σ_{L}^z: $\sigma_{\mathrm{L}}^z = -1$ means that the electric field at a fixed point rotates in the clockwise direction as time evolves [Fig. 4(e)].

The topological properties of the twisted light beam discussed above can be understood by introducing the winding number of the electric field. In general, the winding number of a 2D vector field $\boldsymbol{n} = (n_x, n_y)$ on a closed loop C is defined by

$$
\omega_v[\boldsymbol{n}] \equiv \frac{1}{2\pi} \oint_C \delta_{ij} \epsilon^{\mu\nu} dx_i \frac{n_\mu}{|\boldsymbol{n}|} \frac{\partial}{\partial x_j} \left(\frac{n_\nu}{|\boldsymbol{n}|}\right),
\tag{67}
$$

where ϵ^{ij} is the 2D Levi-Civita symbol, and $|\boldsymbol{n}|$ is supposed to be nonzero on C. The winding number corresponds to the number of times the 2D unit vector $\boldsymbol{n}/|\boldsymbol{n}|$ rotates about the z axis as one traces the contour C. For the electric field given by Eq. (62), the winding number $w_v(\boldsymbol{E})$ is defined on a contour that encloses $r = 0$. Substituting Eq. (62) in (67), we obtain $w_v(\boldsymbol{E}) = -\sigma_{\mathrm{L}}^z m_{\mathrm{L}}^z$. For example, for the electric field with $(\sigma_{\mathrm{L}}^z, m_{\mathrm{L}}^z) = (-1,0), (-1,1), (-1,2)$, and $(-1,-1)$, we have $w_v(\boldsymbol{E}) = 0, 1, 2$, and -1, respectively, which are

consistent with the configurations shown in Fig. 4. The result $w_v(\boldsymbol{E}) = -\sigma_L^z m_L^z$ is also consistent with the fact that the direction of the electric field with $\sigma_L^z = 0$ is spatially uniform even for $m_L^z \neq 0$ and that the whirling direction for $\sigma_L^z = 1$ is opposite to that for $\sigma_L^z = -1$.

B. Charge density

We consider the charge density due to the electric field of the twisted light beam on the disordered surface of the TI. The setup we consider is schematically described in Fig. 3. The induced charge density ρ_e is given by Eq. (39), which can be rewritten as

$$\rho_e(\boldsymbol{x},t) = \frac{1}{\tau} \int_{-\infty}^{\infty} dt' \int d\boldsymbol{x}' \mathcal{D}(\boldsymbol{x}',t') \bar{\rho}_e(\boldsymbol{x} - \boldsymbol{x}', t - t'), \quad (68)$$

$$\bar{\rho}_e(\boldsymbol{x},t) = -2e^2 \nu_e D\tau \boldsymbol{\nabla} \cdot \boldsymbol{E}(\boldsymbol{x},t). \quad (69)$$

By using Eq. (62), $\boldsymbol{\nabla} r = \boldsymbol{r}/r = (\cos \varphi, \sin \varphi)$ and $\boldsymbol{\nabla} \varphi = (\boldsymbol{z} \times \boldsymbol{r})/r^2 = (-\sin \varphi/r, \cos \varphi/r)$, the divergence of the electric field for $\sigma_L^z = \pm 1$ is given by

$$\boldsymbol{\nabla} \cdot \boldsymbol{E} = \left(\frac{\partial \mathcal{E}}{\partial r} - \frac{\sigma_L^z m_L^z \mathcal{E}}{r} \right) \cos \left[(m_L^z + \sigma_L^z)\varphi - \Omega t \right]. \quad (70)$$

Then, $\bar{\rho}_e$ becomes

$$\bar{\rho}_e(\boldsymbol{x},t) = -2e^2 \nu_e D\tau \left(\frac{\partial \mathcal{E}}{\partial r} - \frac{\sigma_L^z m_L^z \mathcal{E}}{r} \right) \cos \left(j_L^z \varphi - \Omega t \right), \quad (71)$$

where $j_L^z \equiv m_L^z + \sigma_L^z$ denotes the total angular momentum of light.

We further simplify Eqs. (68) and (69). First of all, these equations are valid only for $\Omega \tau \ll 1$. This condition means that the period of the oscillation of $\bar{\rho}_e$, which is the same as that of the electric field $T = 2\pi/\Omega$, is much slower than the electron relaxation time τ. On the other hand, the length scale of the spatial variation of $\bar{\rho}_e$ is in the order of the beam waist d_0 [see Eq. (64) and Fig. 4], which is comparable to the wavelength λ of the light. Since λ satisfies $\ell/\lambda = 2\pi \ell \Omega/c_0 = (2\pi \tilde{v}_F/c_0)\Omega\tau \ll 1$, the spatial variation of $\bar{\rho}_e$ is much slower than the mean-free path ℓ, where c_0 is the speed of light and we have used $2\pi \tilde{v}_F \ll c_0$ for realistic TIs [29]. Then, since τ and ℓ determine the decay time and decay length of the diffusion propagator $\mathcal{D}(\boldsymbol{x},t)$, respectively, $\bar{\rho}_e(\boldsymbol{x} - \boldsymbol{x}', t - t')$ in the integrand of Eq. (68) can be approximated as $\bar{\rho}_e(\boldsymbol{x},t)$, and the convolution can be approximately described by

$$\rho_e(\boldsymbol{x},t) \simeq \alpha \bar{\rho}_e(\boldsymbol{x},t), \quad (72)$$

where $\alpha \equiv \frac{1}{\tau} \iint dt \, d\boldsymbol{x} \, \mathcal{D}(\boldsymbol{x},t)$ is a constant coefficient and is estimated by

$$\alpha \simeq \frac{1}{\tau} \int_0^{\tau} dt \int_0^{2\pi} d\phi \int_0^{\ell} r \, dr \, \mathcal{D}. \quad (73)$$

Figure 5 represents the nonlocal charge density due to the twisted light beam ρ_e for a $\sigma_L^z = -1$ and $m_L^z = 0,1,2$, and -1. We find that the distribution of ρ_e depends on the z component of the total angular momentum of light j_L^z. For $j_L^z = 0$ [Fig. 5(b)], the charge density is isotropically induced from the center and the sign of the induced charge changes at $r \sim d_0$. On the other hand, the charge density for nonzero j_L^z distributes anisotropically. The symmetry of
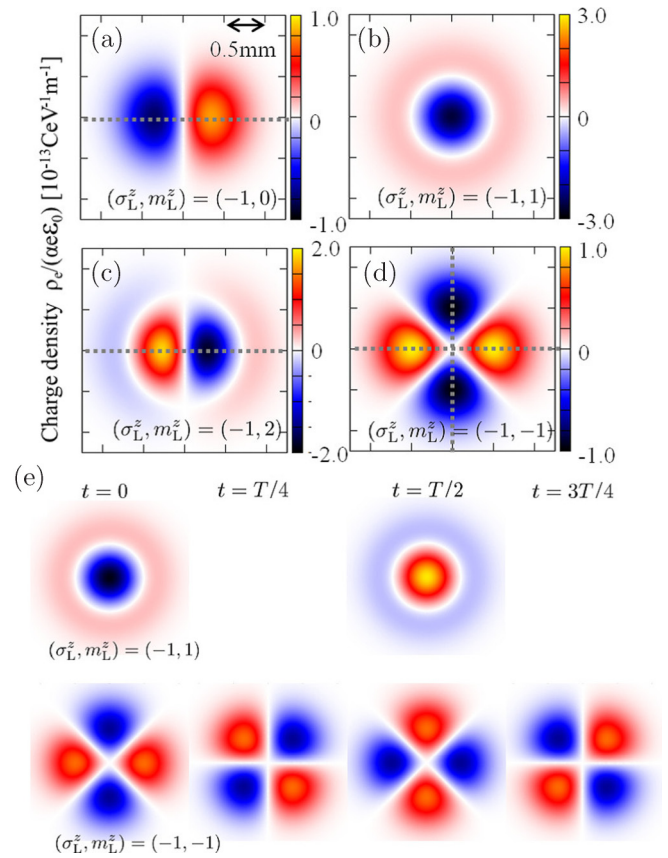

FIG. 5. Snapshots of the charge density induced by the optical twisted light beam with (a) $(\sigma_L^z, m_L^z) = (-1,0)$, (b) $(-1,1)$, (c) $(-1,2)$, and (d) $(-1,-1)$. The dashed lines in (a), (c), and (d) indicate axes of the inversion symmetry. (e) Time evolution of the charge density with $(\sigma_L^z, m_L^z) = (-1,1)$ (top) and $(-1,-1)$ (bottom). In all figures, we use $d_0 = 0.5$ mm, $\epsilon_F = 100$ meV, $\tilde{v}_F = 3 \times 10^5$ m/s, and $\tau = 1 \times 10^{-13}$ s.

the distribution of ρ_e with $|j_L^z| = 1$ [Figs. 5(a) and 5(c)] and $|j_L^z| = 2$ [Fig. 5(d)] are the same as that for the electron wave functions with the p_x and $d_{x^2-y^2}$ orbitals, respectively. The dashed lines in Figs. 5(a), 5(c), and 5(d) indicate the axes of the inversion symmetry of the charge density. As time evolves, the distribution of the induced charge density rotates around the beam center ($j_L^z \neq 0$) or oscillates around the zero value ($j_L^z = 0$) with the frequency of light Ω [see Fig. 5(e)]. The time evolution of the charge density also depends on the total angular momentum of light: When the sign of the total angular momentum is minus (plus), the distribution of the charge density rotates in the clockwise (counterclockwise) direction around the phase singularity during the irradiation. When we turn off the incident light, the charge density diffusively propagates on the disordered surface of the TI with obeying the diffusive equation of motion represented in Eq. (53). Eventually, the induced charge vanishes.

C. Spin density

We turn to discuss the spin density induced by the electric field of the twisted light beam in the same setup as that considered in Sec. V B. As discussed in Sec. IV B,
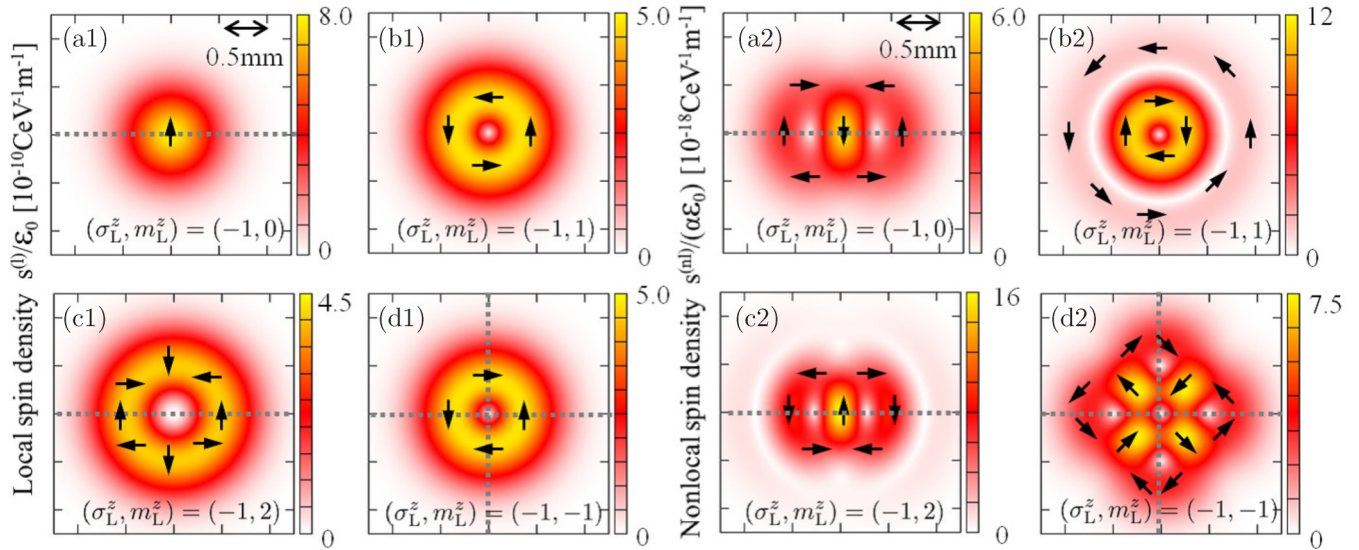
FIG. 6. Snapshots of the spin density induced by the electric field of the optical twisted light beam with (a1) and (a2) $(\sigma_L^z, m_L^z) = (-1, 0)$, (b1) and (b2) $(\sigma_L^z, m_L^z) = (-1, 1)$, (c1) and (c2) $(\sigma_L^z, m_L^z) = (-1, 2)$, and (d1) and (d2) $(\sigma_L^z, m_L^z) = (-1, -1)$. The left (right) panels show the local (nonlocal) spin density. The color map and the direction of the arrow show the magnitude and direction of the spin density, respectively. The parameters are the same as those in Fig. 5.

the induced spin density can be divided into the local and nonlocal ones as $s = s^{(l)} + s^{(nl)}$. The local spin density $s^{(l)}$ is described in Eq. (52) and its snapshots for several m_L^z are shown in Figs. 6(a1)–6(d1). The direction of $s^{(l)}$ is perfectly perpendicular to the electric field. We find that the dynamical vortexlike spin structure is generated by the twisted light beam and the winding number of the local spin density, which is defined by Eq. (67) with $n = s^{(l)}$, is identical to that of the electric field

$$\omega_v[s^{(l)}] = \omega_v[E] = -\sigma_L^z m_L^z \qquad (74)$$

[see Figs. 6(a1)–6(d1) and Figs. 4(a)–4(d)]. On the other hand, the nonlocal spin density $s^{(nl)}$ is proportional to the spatial gradient of the charge density [see the second term of Eq. (46)], and can be estimated by using Eq. (72) as $s^{(nl)} \simeq \frac{\alpha\ell}{2e}(z \times \nabla)\bar{\rho}_e$. The snapshots of $s^{(nl)}$ are shown in Figs. 6(a2)–6(d2). We find that dynamical vortexlike spin structures appear and the spin density becomes zero at the center of the vortex. Here, we note that $s^{(nl)}$ and $\nabla\rho_e$ share the same winding number as they are perfectly perpendicular to each other. Since the winding number $w_v(\nabla\rho_e)$ is 1 (−1) around the maxima and minima (the saddle points) of ρ_e, the centers of the spin vortices locate
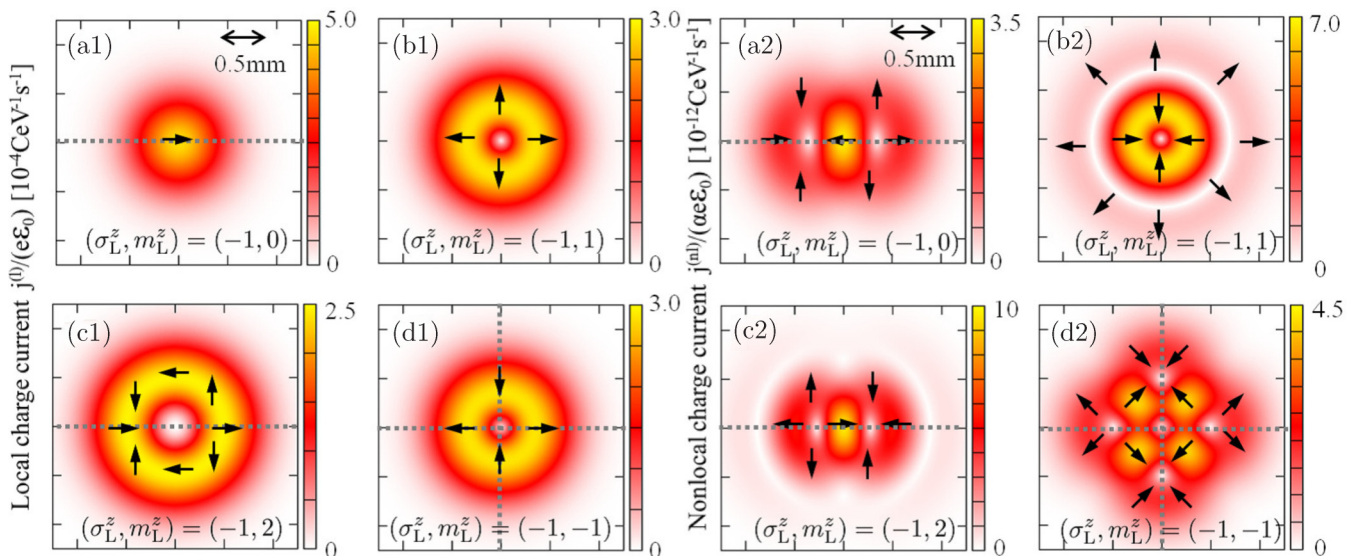

FIG. 7. Snapshots of the charge current density induced by the electric field of the optical twisted light beam with (a1) and (a2) $(\sigma_L^z, m_L^z) = (-1, 0)$, (b1) and (b2) $(\sigma_L^z, m_L^z) = (-1, 1)$, (c1) and (c2) $(\sigma_L^z, m_L^z) = (-1, 2)$, and (d1) and (d2) $(\sigma_L^z, m_L^z) = (-1, -1)$. The left (right) panels show the local (nonlocal) charge current density. The color map and the direction of the arrow show the magnitude and direction of the charge current density, respectively. The parameters are the same as those in Fig. 5.

at the extrema (minima, maxima, and saddle points) of ρ_e, and therefore, they align on the symmetry axis of the distribution of ρ_e (the dotted lines in Fig. 5). For the cases shown in Figs. 6(a2)–6(d2), all spin vortices have the winding number $w_v(s^{(nl)}) = 1$ except for the one at the center of Fig. 6(d2), which corresponds to the saddle point of ρ_e and has the winding number -1. Since $s^{(nl)}$ is related to $\nabla \cdot E$ rather than E, the configuration of the spin vortices depends on the total angular momentum j_L^z. Note, however, that with the parameters for a realistic system, $|s^{(nl)}|/|s^{(l)}|$ is in the order of $\ell^2/d_0^2 \sim 10^{-7}$ and $s^{(nl)}$ is negligibly small as compared with $s^{(l)}$. When we turn off the beam, $s^{(nl)}$ becomes prominent and diffusively propagates. We expect that the photoinduced spin texture can be observed by pump probe technique with the twisted light beam and circularly polarized light beam [4].

D. Charge and spin currents

The profile of the charge current is similar to that of the spin because of the spin momentum locking on the surface of the TI. In Fig. 7, we show the snapshots of the charge current for various angular momenta of light, where the left (right) four panels depict the local (nonlocal) components. Reflecting the relation $j \parallel z \times s$, the magnitude of $j^{(l,nl)}$ has the same profile as that of $|s^{(l,nl)}|$, while the direction of $j^{(l,nl)}$ is obtained by rotating $s^{(l,nl)}$ by $-\pi/2$ about the z axis. As in the case of the spin density, the local (nonlocal) part of the charge current is related to E ($\nabla \cdot E$) and hence its configuration is mainly determined by m_L^z (j_L^z).

Figure 8 shows the light-induced spin current. As one can see from Eq. (58), the magnitude of the spin current is proportional to $|\rho_e|$ and the direction of the spin and its current perfectly perpendicular to each other. These properties also come from the spin-momentum locking on the surface of the TI.
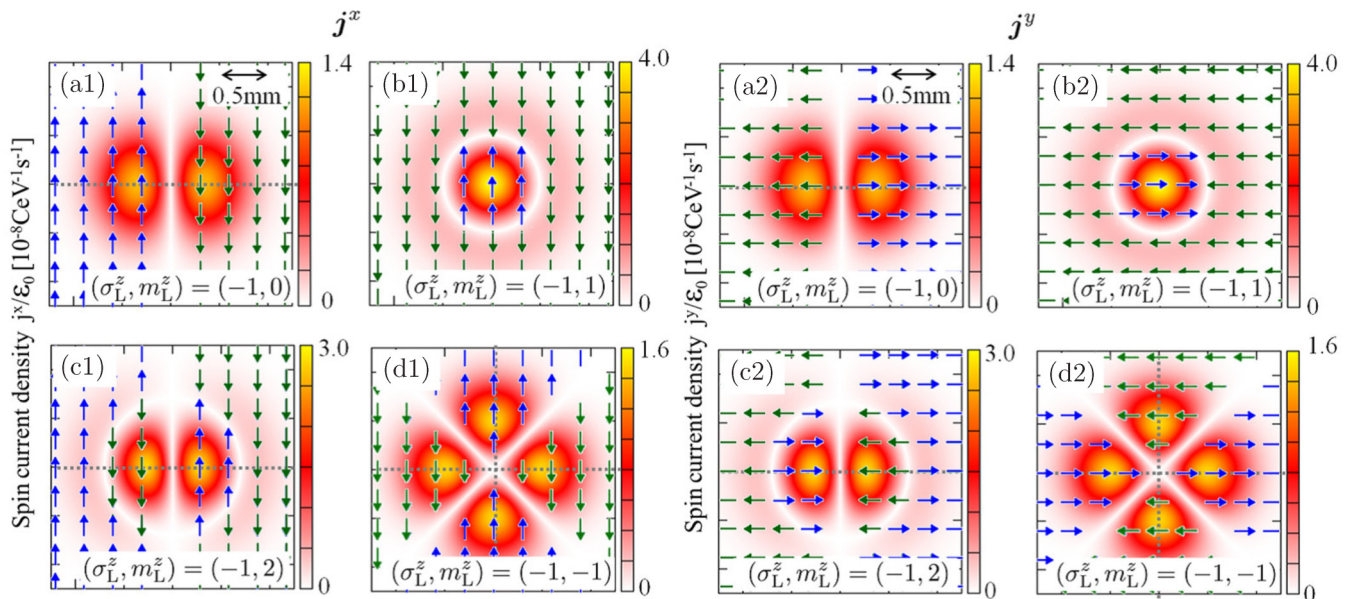
We find that the spatial profile of the spin current is different from that of the (spin-polarized) charge current, which are shown in Figs. 8 and 7, respectively. In fact, they are related to each other via Eq. (60), and only the nonlocal charge current couples to the spin current.

VI. CONCLUSION

We study the charge density, the spin density, the charge current density, and the spin current density induced by a twisted light beam irradiated on a disordered surface of a doped TI by using the Keldysh-Green's function method. We have discussed the responses of charge and spin to the space-time-dependent electric field. The obtained results are summarized in Table I. The effect of the electric field on the electric charge is twofold. First, it induces a charge current along the direction of the electric field. Second, the inhomogeneity of the electric field causes a gradient of the charge density, which then leads to a diffusive charge current. We call the former the local charge current and the latter the nonlocal charge current, based on whether the charge current depends only on the local electric field or is affected by the nonlocal one. Since the spin and momentum of electrons on a surface of a TI are locked to be perpendicular to each other, the emergence of the charge current implies that the spin density is induced in the perpendicular direction to the charge current. Our calculation based on the linear response theory gives the analytic description for the local and nonlocal spin densities as well as the local and nonlocal charge current densities. We also find that the induced charge density also gives rise to a spin current, which is related to the nonlocal part of the charge current via Eq. (60).

By taking into account the spatial and temporal configurations of the electric field associated with a twisted light beam, we have shown that various types of spin vortices arise.

FIG. 8. Snapshots of the spin current density induced by the optical twisted light beam with (a1) and (a2) $(\sigma_L^z, m_L^z) = (-1,0)$, (b1) and (b2) $(\sigma_L^z, m_L^z) = (-1,1)$, (c1) and (c2) $(\sigma_L^z, m_L^z) = (-1,2)$, and (d1) and (d2) $(\sigma_L^z, m_L^z) = (-1,-1)$. The left (right) panels show current of the x (y) component of spin. The color map shows the magnitude of the spin current density. The blue and green arrows show the direction of the flow of the spin. As in the case of the charge density, the distribution of the spin current depends on the total angular momentum of the twisted light beam. The parameters are the same as those in Fig. 5.

TABLE II. In the distribution of the nonlocal part of s and j, several vortices appear, each of which has the winding number $+1$ or -1. The configuration of the vortices is determined by the total angular momentum of light $j_L^z = \sigma_L^z + m_L^z$.

	s	j	Winding number $\omega_v[s], \omega_v[j]$
Local	$z \times E$	E	$-\sigma_L^z m_L^z$
Nonlocal	$(z \times \nabla)\nabla \cdot \langle E \rangle_D$	$\nabla(\nabla \cdot \langle E \rangle_D)$	± 1

Since the local spin density is perpendicular to the electric field, their winding numbers are identical and determined by the product of the spin and orbital angular momentum of the twisted light beam (Table II). In this paper, we have assumed that the time (length) scale of the diffusion of electrons is much faster (shorter) than those of incident light. In such a situation, we can approximate the nonlocal electric field with the bare electric field, and the nonlocal quantities are described using the divergence of the electric field. Thus, the configurations of the nonlocal densities and currents are determined by the total angular momentum of the twisted light beam.

APPENDIX A: MODIFICATION OF v_F

The Fermi velocity of the Hamiltonian on the surface of the TI is modified from the contributions of the impurity scatterings in the absence of electromagnetic fields [30,31,36,37]. Following, we will demonstrate the modification of v_F in the presence of electromagnetic fields.

The Green's function including the electromagnetic fields with considering impurity scatterings is given by

$$\hat{g}_{k,\omega}^r(A_{em}) = [\hbar\omega + \epsilon_F - \hbar v_F \hat{\sigma} \cdot (k \times z) + e v_F \hat{\sigma} \cdot (A_{em} \times z) - \hat{\Sigma}_{k,\omega}^r(A_{em})]^{-1}. \tag{A1}$$

Here, the self-energy $\hat{\Sigma}_{k,\omega}^r(A_{em})$ is given by

$$\hat{\Sigma}_{k,\omega}^r(A_{em}) = n_i \sum_{k'} |u_{k-k'}|^2 \hat{g}_{k',\omega}^r(A_{em}) = n_i \sum_q |u_q|^2 \hat{g}_{k+q,\omega}^r(A_{em}). \tag{A2}$$

We assume that the Green's function can be expanded with k and A_{em} as

$$\hat{\Sigma}_{k,\omega}^r(A_{em}) = n_i \sum_q |u_q|^2 \left[\hat{g}_{q,\omega}^r(0) + k \cdot \frac{\partial}{\partial k} \hat{g}_{k+q,\omega}^r(A_{em}) \Big|_{A_{em}=k=0} + A_{em} \cdot \frac{\partial}{\partial A_{em}} \hat{g}_{k+q,\omega}^r(A_{em}) \Big|_{A_{em}=k=0} \right] + O(k^2, A_{em}^2, kA_{em}). \tag{A3}$$

The above functions are given by using $\lim_{q\to\infty} u_q = 0$ [30,31] as

$$\frac{\partial}{\partial k} \hat{g}_{k+q,\omega}^r(A_{em}) \Big|_{A_{em}=k=0} = \hat{g}_{q,\omega}^r(0) \left[\hbar v_F(z \times \hat{\sigma}) + \frac{\partial \hat{\Sigma}_{q,\omega}^r(0)}{\partial q} \right] \hat{g}_{q,\omega}^r(0), \tag{A4}$$

$$\frac{\partial}{\partial A_{em}} \hat{g}_{k+q,\omega}^r(A_{em}) \Big|_{A_{em}=k=0} = \hat{g}_{q,\omega}^r(0) \left[-e v_F(z \times \hat{\sigma}) + \frac{\partial \hat{\Sigma}_{q,\omega}^r(A_{em})}{\partial A_{em}} \Big|_{A_{em}=0} \right] \hat{g}_{q,\omega}^r(0), \tag{A5}$$

and the self-energy becomes

$$\hat{\Sigma}_{k,\omega}^r(A_{em}) = \hat{\Sigma}_{0,k,\omega}(0) + \hat{\Sigma}_{\perp,k,\omega}(0) + \hat{\Sigma}_{\perp,0,\omega}(A_{em}) + O(k^2, A_{em}^2, kA_{em}), \tag{A6}$$

with

$$\hat{\Sigma}_{0,k,\omega}^r(0) = n_i \sum_q |u_q|^2 \hat{g}_{q,\omega}^r(0), \tag{A7}$$

$$\hat{\Sigma}_{\perp,k,\omega}^r(0) = n_i \sum_q |u_q|^2 \hat{g}_{q,\omega}^r(0) k \cdot \left[\hbar v_F(z \times \hat{\sigma}) + \frac{\partial \hat{\Sigma}_{q,\omega}^r(0)}{\partial q} \right] \hat{g}_{q,\omega}^r(0), \tag{A8}$$

$$\hat{\Sigma}_{\perp,0,\omega}^r(A_{em}) = n_i \sum_q |u_q|^2 \hat{g}_{q,\omega}^r(0) A_{em} \cdot \left[-e v_F(z \times \hat{\sigma}) + \frac{\partial \hat{\Sigma}_{q,\omega}^r(A_{em})}{\partial A_{em}} \Big|_{A_{em}=0} \right] \hat{g}_{q,\omega}^r(0). \tag{A9}$$

$\hat{\Sigma}^{\mathrm{r}}_{0,\mathbf{k},\omega}(\mathbf{0})$ and $\hat{\Sigma}^{\mathrm{r}}_{\perp,\mathbf{k},\omega}(\mathbf{0})$ have been calculated in the previous works [30,31]. We calculate $\hat{\Sigma}^{\mathrm{r}}_{\perp,\mathbf{0},\omega}(\mathbf{A}_{\mathrm{em}})$ within the same formalism of these works [30,31]. We suppose that $\hat{\Sigma}^{\mathrm{r}}_{\perp,\mathbf{0},\omega}(\mathbf{A}_{\mathrm{em}})$ is obtained by the following form: $\hat{\Sigma}^{\mathrm{r}}_{\perp,\mathbf{0},\omega}(\mathbf{A}_{\mathrm{em}}) = -ev_{\mathrm{F}} d_{ij} A_{\mathrm{em},i} \hat{\sigma}_j$ with a second rank tensor d_{ij}. Substituting $\hat{\Sigma}^{\mathrm{r}}_{\perp,\mathbf{0},\omega}(\mathbf{A}_{\mathrm{em}}) = -ev_{\mathrm{F}} d_{ij} A_{\mathrm{em},i} \hat{\sigma}_j$ into the above equation, we can calculate as

$$\hat{\Sigma}^{\mathrm{r}}_{\perp,\mathbf{0},\omega}(\mathbf{A}_{\mathrm{em}}) = n_{\mathrm{i}} \sum_{\mathbf{q}} |u_{\mathbf{q}}|^2 \hat{g}^{\mathrm{r}}_{\mathbf{q},\omega}(\mathbf{0}) \sum_{\ell,j=x,y} A_{\mathrm{em},\ell} [-ev_{\mathrm{F}}(\mathbf{z}\times\hat{\boldsymbol{\sigma}})_\ell - ev_{\mathrm{F}} d_{\ell j} \hat{\sigma}_j] \hat{g}^{\mathrm{r}}_{\mathbf{q},\omega}(\mathbf{0}) = n_{\mathrm{i}} \sum_{\ell,j=x,y} A_{\mathrm{em},\ell} \frac{u_0^2 ev_{\mathrm{F}}}{4\pi\hbar^2 v_{\mathrm{F}}^2} \hat{\sigma}_j [\epsilon_{\ell z j} + d_{\ell j}]. \tag{A10}$$

Therefore, we obtain

$$d_{\ell j} = -\frac{n_{\mathrm{i}} u_0^2}{4\pi\hbar^2 v_{\mathrm{F}}^2} [\epsilon_{\ell z j} + d_{\ell j}]$$

and $d_{\ell j} = \xi/(1+\xi)\epsilon_{\ell j z}$. As a result, the self-energy becomes

$$\hat{\Sigma}^{\mathrm{r}}_{\perp,\mathbf{0},\omega}(\mathbf{A}_{\mathrm{em}}) = \frac{-\xi}{1+\xi}\epsilon_{\ell j z} ev_{\mathrm{F}} A_{\mathrm{em},i} \hat{\sigma}_j.$$

From the result, Eq. (A1) is modified within $O(k^2, A_{\mathrm{em}}^2, k A_{\mathrm{em}})$ as

$$\hat{g}^{\mathrm{r}}_{\mathbf{k},\omega}(\mathbf{A}_{\mathrm{em}}) = [\hbar\omega + \epsilon_{\mathrm{F}} - \hbar\tilde{v}_{\mathrm{F}}\hat{\boldsymbol{\sigma}}\cdot(\mathbf{k}\times\mathbf{z}) + e\tilde{v}_{\mathrm{F}}\hat{\boldsymbol{\sigma}}\cdot(\mathbf{A}_{\mathrm{em}}\times\mathbf{z}) + i\eta]^{-1}. \tag{A11}$$

From the above equation, we see that the Fermi velocity in Eq. (4) is also replaced by $\tilde{v}_{\mathrm{F}}$.

APPENDIX B: DERIVATION OF $\hat{I}_\mu$

We estimate $\hat{I}_\mu$ in Eq. (26) by expanding with respect to $\mathbf{q}$ and Ω within $q\ell \ll 1$ and $\Omega\tau \ll 1$ and by using the Green's function

$$\hat{g}^{\mathrm{r}}_{\mathbf{k}\pm\frac{\mathbf{q}}{2},\pm\frac{\Omega}{2}} = \hat{g}^{\mathrm{r}}_{\mathbf{k}} \pm \frac{1}{2}\left[\sum_{\xi=x,y} q_\xi \frac{\partial \hat{g}^{\mathrm{r}}_{\mathbf{k}}}{\partial k_\xi} + \Omega \frac{\partial \hat{g}^{\mathrm{r}}_{\mathbf{k},\omega}}{\partial\omega}\bigg|_{\omega\to 0}\right] + \frac{1}{8}\sum_{\xi,\xi'=x,y} q_\xi q_{\xi'} \frac{\partial^2 \hat{g}^{\mathrm{r}}_{\mathbf{k}}}{\partial k_\xi \partial k_{\xi'}} + O(q^3, q\Omega, \Omega^2),$$

where we use the shorthand notation $\hat{g}^{\mathrm{r}}_{\mathbf{k}} \equiv \hat{g}^{\mathrm{r}}_{\mathbf{k},\omega=0}$. $\hat{I}_\mu$ is decomposed into four terms as

$$\hat{I}_\mu \equiv \hat{I}^{(0)}_\mu + \Omega \hat{I}^{(1)}_\mu + \sum_{\xi=x,y} q_\xi \hat{I}^{(2)}_{\mu\xi} + \sum_{\xi,\xi'=x,y} q_\xi q_{\xi'} \hat{I}^{(3)}_{\mu\xi\xi'}, \tag{B1}$$

$$\hat{I}^{(0)}_\mu = \sum_{\mathbf{k}} \hat{g}^{\mathrm{r}}_{\mathbf{k}} \hat{\sigma}_\mu \hat{g}^{\mathrm{a}}_{\mathbf{k}}, \tag{B2}$$

$$\hat{I}^{(1)}_\mu = \frac{1}{2}\sum_{\mathbf{k}}\left(\hat{g}^{\mathrm{r}}_{\mathbf{k}} \hat{\sigma}_\mu \frac{\partial \hat{g}^{\mathrm{a}}_{\mathbf{k},\omega}}{\partial\omega}\bigg|_{\omega\to 0} - \mathrm{H.c}\right), \tag{B3}$$

$$\hat{I}^{(2)}_{\mu\xi} = \frac{1}{2}\sum_{\mathbf{k}}\left(\hat{g}^{\mathrm{r}}_{\mathbf{k}} \hat{\sigma}_\mu \frac{\partial \hat{g}^{\mathrm{a}}_{\mathbf{k}}}{\partial k_\xi} - \mathrm{H.c}\right), \tag{B4}$$

$$\hat{I}^{(3)}_{\mu\xi\xi'} = \frac{1}{8}\sum_{\mathbf{k}}\left(\hat{g}^{\mathrm{r}}_{\mathbf{k}} \hat{\sigma}_\mu \frac{\partial^2 \hat{g}^{\mathrm{a}}_{\mathbf{k}}}{\partial k_\xi \partial k_{\xi'}} + \frac{\partial^2 \hat{g}^{\mathrm{r}}_{\mathbf{k}}}{\partial k_\xi \partial k_{\xi'}} \hat{\sigma}_\mu \hat{g}^{\mathrm{a}}_{\mathbf{k}} - 2\frac{\partial \hat{g}^{\mathrm{r}}_{\mathbf{k}}}{\partial k_\xi} \hat{\sigma}_\mu \frac{\partial \hat{g}^{\mathrm{a}}_{\mathbf{k}}}{\partial k_{\xi'}}\right). \tag{B5}$$

In Appendix F, we list useful formulas for the integral of the Green's functions, which are used in the following calculations.

1. Calculation of $\hat{I}^{(0)}_{\mu=x,y,z}$

First, to calculate $\hat{I}^{(0)}_{\mu=x,y,z}$ in Eq. (B2), we divide $\hat{g}^{\mathrm{r}}_{\mathbf{k}} \hat{\sigma}_\mu \hat{g}^{\mathrm{a}}_{\mathbf{k}}$ into the even and odd functions of $\mathbf{k}$:

$$\hat{g}^{\mathrm{r}}_{\mathbf{k}} \hat{\sigma}_\mu \hat{g}^{\mathrm{a}}_{\mathbf{k}} = D^{\mathrm{r}} D^{\mathrm{a}} \hat{\mathcal{Q}} \hat{\sigma}_\mu \hat{\mathcal{Q}}^\dagger, \tag{B6}$$

where D^{r}, $D^{\mathrm{a}} = [D^{\mathrm{r}}]^*$, $\hat{\mathcal{Q}}$, $\hat{\mathcal{Q}}^\dagger$, h, and h^* are defined by

$$D^{\mathrm{r}} \equiv \left(h^2 - \hbar^2\tilde{v}_{\mathrm{F}}^2 k^2\right)^{-1}, \tag{B7}$$

$$\hat{\mathcal{Q}} \equiv h + \hbar\tilde{v}_{\mathrm{F}}\mathbf{k}\cdot(\mathbf{z}\times\hat{\boldsymbol{\sigma}}), \tag{B8}$$

$$\hat{\mathcal{Q}}^\dagger \equiv h^* + \hbar\tilde{v}_{\mathrm{F}}\mathbf{k}\cdot(\mathbf{z}\times\hat{\boldsymbol{\sigma}}), \tag{B9}$$

$$h \equiv \epsilon_{\mathrm{F}} + i\eta, \tag{B10}$$

$$h^* \equiv \epsilon_{\mathrm{F}} - i\eta. \tag{B11}$$

D^{r} and D^{a} are the even functions of $\boldsymbol{k}$. $\hat{\mathcal{Q}}\hat{\sigma}_\mu \hat{\mathcal{Q}}^\dagger$ is represented by

$$\hat{\mathcal{Q}}\hat{\sigma}_\mu \hat{\mathcal{Q}}^\dagger = \left[|h|^2 \hat{\sigma}_\mu + \hbar^2 \tilde{v}_{\mathrm{F}}^2 \sum_{\ell,\ell'=x,y} k_\ell k_{\ell'} (\boldsymbol{z}\times\hat{\boldsymbol{\sigma}})_\ell \hat{\sigma}_\mu (\boldsymbol{z}\times\hat{\boldsymbol{\sigma}})_{\ell'}\right] + \hbar\tilde{v}_{\mathrm{F}} \sum_{\ell=x,y} [hk_\ell \hat{\sigma}_\mu (\boldsymbol{z}\times\hat{\boldsymbol{\sigma}})_\ell + h^* k_\ell (\boldsymbol{z}\times\hat{\boldsymbol{\sigma}})_\ell \hat{\sigma}_\mu]. \tag{B12}$$

The first and second terms are corresponding to the even and odd functions of $\boldsymbol{k}$, respectively. In the following calculation, we simply assume that the surface of the TI is isotropic as a function of $\boldsymbol{k}$: $k_x^2 = k_y^2 = k^2/2$. By taking an average over the direction of $\boldsymbol{k}$, $\langle \ldots \rangle_k$, in Eq. (B12) and using $\langle k_\ell \rangle_k = 0$ and $\langle k_\ell k_{\ell'} \rangle_k = \frac{1}{2}k^2 \delta_{\ell\ell'}$, we obtain

$$\langle \hat{\mathcal{Q}}\hat{\sigma}_\mu \hat{\mathcal{Q}}^\dagger \rangle_k = |h|^2 \hat{\sigma}_\mu + \frac{1}{2}\hbar^2 \tilde{v}_{\mathrm{F}}^2 k^2 \sum_{\ell=x,y} (\boldsymbol{z}\times\hat{\boldsymbol{\sigma}})_\ell \hat{\sigma}_\mu (\boldsymbol{z}\times\hat{\boldsymbol{\sigma}})_\ell. \tag{B13}$$

The second term in the above equation becomes

$$\sum_{\ell=x,y} (\boldsymbol{z}\times\hat{\boldsymbol{\sigma}})_\ell \hat{\sigma}_\mu (\boldsymbol{z}\times\hat{\boldsymbol{\sigma}})_\ell = \sum_{\ell=x,y} (2\delta_{\ell\mu}\hat{\sigma}_\ell - \delta_{\ell\ell}\hat{\sigma}_\mu) \tag{B14}$$

$$= -2\delta_{\mu z}\hat{\sigma}_z. \tag{B15}$$

Thus, we obtain $\hat{I}_\mu^{(0)}$ as

$$\hat{I}_{\mu=x,y}^{(0)} = |h|^2 \sum_{\boldsymbol{k}} |D^{\mathrm{r}}|^2 \hat{\sigma}_\mu, \tag{B16}$$

$$\hat{I}_z^{(0)} = \sum_{\boldsymbol{k}} \left(|h|^2 - \hbar^2 \tilde{v}_{\mathrm{F}}^2 k^2\right)|D^{\mathrm{r}}|^2 \hat{\sigma}_z. \tag{B17}$$

The integral of Eq. (B16) is obtained by

$$\sum_{\boldsymbol{k}} |D^{\mathrm{r}}|^2 = \frac{1}{2\pi}\int_0^\infty \frac{k\,dk}{[h^2 - \hbar^2 \tilde{v}_{\mathrm{F}}^2 k^2][(h^*)^2 - \hbar^2 \tilde{v}_{\mathrm{F}}^2 k^2]} = \frac{\nu_e}{2\epsilon_{\mathrm{F}}}\int_0^\infty \frac{dx}{[h^2 - x][(h^*)^2 - x]}$$

$$= \frac{\nu_e}{2\epsilon_{\mathrm{F}}[h^2 - (h^*)^2]}\int_0^\infty dx\left[\frac{1}{x - h^2} - \frac{1}{x - (h^*)^2}\right], \tag{B18}$$

where $\nu_e = \frac{\epsilon_{\mathrm{F}}}{2\pi\hbar^2 \tilde{v}_{\mathrm{F}}^2}$ is the density of states on the surface. Here, the above integral is given by

$$\int_0^\infty dx\left[\frac{1}{x - h^2} - \frac{1}{x - (h^*)^2}\right] = \log\frac{x - h^2}{x - (h^*)^2}\bigg|_{x\to 0}^{x\to\infty} = i[\arg(x - h^2) - \arg[x - (h^*)^2]]_{x\to 0}^{x\to\infty}. \tag{B19}$$

In the above equation, we have used $\log z = \log|z| + i\arg z$, where $z = a + ib = |z|e^{i\theta}$, $a,b \in \mathbb{R}$. Here, $\theta = \arg z$ is

$$\theta = \begin{cases} \tan^{-1}(b/a) & (a > 0 \quad \text{and} \quad b > 0), \\ \pi + \tan^{-1}(b/a) & (a < 0), \\ 2\pi + \tan^{-1}(b/a) & (a > 0 \quad \text{and} \quad b < 0). \end{cases} \tag{B20}$$

Thus, $\arg(x - h^2)|_{x\to 0}^{x\to\infty} = \pi + O(\hbar/\epsilon_{\mathrm{F}}\tau)$, $\arg[x - (h^*)^2]|_{x\to 0}^{x\to\infty} = -\pi + O(\hbar/\epsilon_{\mathrm{F}}\tau)$, and

$$\log\frac{x - h^2}{x - (h^*)^2}\bigg|_{x\to 0}^{x\to\infty} \simeq 2i\pi \tag{B21}$$

are satisfied. We have $\sum_{\boldsymbol{k}} |D^{\mathrm{r}}|^2 = \frac{\pi\nu_e}{4\eta\epsilon_{\mathrm{F}}^2} + O(\hbar/\epsilon_{\mathrm{F}}\tau)$ and

$$\hat{I}_{\mu=x,y}^{(0)} = \frac{\pi\nu_e}{4\eta}\hat{\sigma}_\mu. \tag{B22}$$

Equation (B17) can be estimated around the Fermi energy $k \to k_{\mathrm{F}} \equiv \epsilon_{\mathrm{F}}/(\hbar\tilde{v}_{\mathrm{F}})$ as

$$\hat{I}_z^{(0)} \sim \left(|h|^2 - \hbar^2 \tilde{v}_{\mathrm{F}}^2 k_{\mathrm{F}}^2\right)\sum_{\boldsymbol{k}} |D^{\mathrm{r}}|^2 \hat{\sigma}_z = O\left(\frac{\hbar}{\epsilon_{\mathrm{F}}\tau}\right). \tag{B23}$$

2. Calculation of $\hat{I}^{(1)}_{\mu=x,y,z}$

To calculate $\hat{I}^{(1)}_{\mu=x,y,z}$ in Eq. (B3), we divide $\hat{g}^{\text{r}}_{\boldsymbol{k}}\hat{\sigma}_\mu \frac{\partial \hat{g}^{\text{a}}_{k,\omega}}{\partial \omega}|_{\omega\to 0} = -\hbar \hat{g}^{\text{r}}_{\boldsymbol{k}}\hat{\sigma}_\mu (\hat{g}^{\text{a}}_{\boldsymbol{k}})^2 = -\hbar D^{\text{r}}(D^{\text{a}})^2 \hat{\mathcal{Q}}\hat{\sigma}_\mu (\hat{\mathcal{Q}}^\dagger)^2$ into the even and odd functions of $\boldsymbol{k}$. Here, $(\hat{\mathcal{Q}}^\dagger)^2$ and $\hat{\mathcal{Q}}\hat{\sigma}_\mu (\hat{\mathcal{Q}}^\dagger)^2$ become

$$(\hat{\mathcal{Q}}^\dagger)^2 = \left[(h^*)^2 + \hbar^2 \tilde{v}_{\text{F}}^2 k^2\right] + 2h^*\hbar \tilde{v}_{\text{F}} k_\ell (\boldsymbol{z}\times\hat{\boldsymbol{\sigma}})_\ell, \tag{B24}$$

$$\hat{\mathcal{Q}}\hat{\sigma}_\mu (\hat{\mathcal{Q}}^\dagger)^2 = \left[h\left\{(h^*)^2 + \hbar^2 \tilde{v}_{\text{F}}^2 k^2\right\}\hat{\sigma}_\mu + 2h^*\hbar^2 \tilde{v}_{\text{F}}^2 k_\ell k_{\ell'}(\boldsymbol{z}\times\hat{\boldsymbol{\sigma}})_\ell \hat{\sigma}_\mu (\boldsymbol{z}\times\hat{\boldsymbol{\sigma}})_{\ell'}\right]$$
$$+ \left[2|h|^2\hbar \tilde{v}_{\text{F}} k_\ell (\boldsymbol{z}\times\hat{\boldsymbol{\sigma}})_\ell \hat{\sigma}_\mu \hat{\sigma}_\mu + \left\{(h^*)^2 + \hbar^2 \tilde{v}_{\text{F}}^2 k^2\right\}\hbar \tilde{v}_{\text{F}} k_\ell (\boldsymbol{z}\times\hat{\boldsymbol{\sigma}})_\ell \hat{\sigma}_\mu\right]. \tag{B25}$$

The first and second terms of the above equations are the even and odd functions of $\boldsymbol{k}$. Then, we have

$$\langle \hat{\mathcal{Q}}\hat{\sigma}_\mu (\hat{\mathcal{Q}}^\dagger)^2\rangle_k = h\left\{(h^*)^2 + \hbar^2 \tilde{v}_{\text{F}}^2 k^2\right\}\hat{\sigma}_\mu \quad (\mu = x,y), \tag{B26}$$

$$\langle \hat{\mathcal{Q}}\hat{\sigma}_z (\hat{\mathcal{Q}}^\dagger)^2\rangle_k = h\left\{(h^*)^2 + \hbar^2 \tilde{v}_{\text{F}}^2 k^2\right\}\hat{\sigma}_z - 2h^*\hbar^2 \tilde{v}_{\text{F}}^2 k^2 \hat{\sigma}_z \quad (\mu = z), \tag{B27}$$

from which $\hat{I}^{(1)}_\mu = -\frac{\hbar}{2}\sum_{\boldsymbol{k}}[\hat{g}^{\text{r}}_{\boldsymbol{k}}\hat{\sigma}_\mu (\hat{g}^{\text{a}}_{\boldsymbol{k}})^2 - \text{H.c.}]$ is obtained by

$$\hat{I}^{(1)}_{\mu=x,y} = -\frac{\hbar}{2}\left\{h\sum_{\boldsymbol{k}} D^{\text{r}}(D^{\text{a}})^2\left[(h^*)^2 + \hbar^2 \tilde{v}_{\text{F}}^2 k^2\right]\hat{\sigma}_\mu - \text{H.c.}\right\}$$
$$= -\frac{\hbar}{2}\left[\frac{v_e}{8\eta^2}\left(i\pi - \frac{2\eta^2}{\epsilon_{\text{F}}^2}\right)\left(1 + i\frac{\eta}{\epsilon_{\text{F}}}\right) - \text{c.c.}\right]\hat{\sigma}_\mu + O\left(\frac{\hbar}{\epsilon_{\text{F}}\tau}\right) = \frac{-i\hbar\pi v_e}{8\eta^2}\hat{\sigma}_\mu + O\left(\frac{\hbar}{\epsilon_{\text{F}}\tau}\right), \tag{B28}$$

$$\hat{I}^{(1)}_z = -\frac{\hbar}{2}\left\{\sum_{\boldsymbol{k}} D^{\text{r}}(D^{\text{a}})^2\left[h(h^*)^2 + (h - 2h^*)\hbar^2 \tilde{v}_{\text{F}}^2 k^2\right]\hat{\sigma}_\mu - \text{H.c.}\right\}$$
$$= -\frac{\hbar}{2}\left[\frac{-i\pi v_e}{4\epsilon_{\text{F}}^2}\left(1 + i\frac{\eta}{\epsilon_{\text{F}}}\right) - \text{c.c.}\right]\hat{\sigma}_z + O\left(\frac{\hbar}{\epsilon_{\text{F}}\tau}\right) = \frac{i\hbar\pi v_e}{4\epsilon_{\text{F}}^2}\hat{\sigma}_\mu + O\left(\frac{\hbar}{\epsilon_{\text{F}}\tau}\right). \tag{B29}$$

3. Calculation of $\hat{I}^{(2)}_{\mu(=x,y,z)\xi}$

$\frac{\partial \hat{g}^{\text{r}}_{\boldsymbol{k}}}{\partial k_\xi}$ is given by

$$\frac{\partial \hat{g}^{\text{r}}_{\boldsymbol{k}}}{\partial k_\xi} = \hbar \tilde{v}_{\text{F}}(\boldsymbol{z}\times\hat{\boldsymbol{\sigma}})_\xi D^{\text{r}} + 2\hbar^2 \tilde{v}_{\text{F}}^2 k_\xi \hat{\mathcal{Q}}(D^{\text{r}})^2. \tag{B30}$$

By using Eq. (B30), $\langle \frac{\partial \hat{g}^{\text{r}}_{\boldsymbol{k}}}{\partial k_\xi}\hat{\sigma}_\mu \hat{g}^{\text{a}}_{\boldsymbol{k}}\rangle_k$ becomes

$$\left\langle \frac{\partial \hat{g}^{\text{r}}_{\boldsymbol{k}}}{\partial k_\xi}\hat{\sigma}_\mu \hat{g}^{\text{a}}_{\boldsymbol{k}}\right\rangle_k = \left\langle \left[\hbar \tilde{v}_{\text{F}}(\boldsymbol{z}\times\hat{\boldsymbol{\sigma}})_\xi D^{\text{r}} + 2\hbar^2 \tilde{v}_{\text{F}}^2 k_\xi \hat{\mathcal{Q}}(D^{\text{r}})^2\right]\hat{\sigma}_\mu D^{\text{a}}\hat{\mathcal{Q}}^\dagger\right\rangle_k = \left\langle \hbar \tilde{v}_{\text{F}}(\boldsymbol{z}\times\hat{\boldsymbol{\sigma}})_\xi \hat{\sigma}_\mu \langle \hat{\mathcal{Q}}^\dagger\rangle_k |D^{\text{r}}|^2 + 2\hbar^2 \tilde{v}_{\text{F}}^2 \langle k_\xi \hat{\mathcal{Q}}\hat{\sigma}_\mu \hat{\mathcal{Q}}^\dagger\rangle_k (D^{\text{r}})^2 D^{\text{a}}\right\rangle_k. \tag{B31}$$

Here, $\langle \hat{\mathcal{Q}}^\dagger\rangle_k$ and $\langle k_\xi \hat{\mathcal{Q}}\hat{\sigma}_\mu \hat{\mathcal{Q}}^\dagger\rangle_k$ are given by

$$\langle \hat{\mathcal{Q}}^\dagger\rangle_k = h^*, \tag{B32}$$

$$\langle k_\xi \hat{\mathcal{Q}}\hat{\sigma}_\mu \hat{\mathcal{Q}}^\dagger\rangle_k = \hbar \tilde{v}_{\text{F}}\langle k_\xi k_\ell\rangle_k \{h\hat{\sigma}_\mu (\boldsymbol{z}\times\hat{\boldsymbol{\sigma}})_\ell + h^*(\boldsymbol{z}\times\hat{\boldsymbol{\sigma}})_\ell \hat{\sigma}_\mu\} = \frac{\hbar \tilde{v}_{\text{F}}}{2}k^2\epsilon_{\xi z u}(h\hat{\sigma}_\mu \hat{\sigma}_u + h^*\hat{\sigma}_u \hat{\sigma}_\mu). \tag{B33}$$

$\hat{I}^{(2)}_{\mu\xi}$ in Eq. (B4) is given by

$$\hat{I}^{(2)}_{\mu\xi} = \frac{\hbar \tilde{v}_{\text{F}}}{2}\epsilon_{\xi z u}\sum_{\boldsymbol{k}}\left[|D^{\text{r}}|^2(h\hat{\sigma}_\mu \hat{\sigma}_u - h^*\hat{\sigma}_u \hat{\sigma}_\mu) + \hbar^2 \tilde{v}_{\text{F}}^2 k^2 |D^{\text{r}}|(D^{\text{a}} - D^{\text{r}})(h\hat{\sigma}_\mu \hat{\sigma}_u + h^*\hat{\sigma}_u \hat{\sigma}_\mu)\right]. \tag{B34}$$

Here, $h\hat{\sigma}_\mu \hat{\sigma}_u \pm h^*\hat{\sigma}_u \hat{\sigma}_\mu$ can be transformed as

$$h\hat{\sigma}_\mu \hat{\sigma}_u - h^*\hat{\sigma}_u \hat{\sigma}_\mu = 2i\eta\delta_{\mu u} + 2i\epsilon_{\text{F}}\epsilon_{\mu u \nu}\hat{\sigma}_\nu, \tag{B35}$$

$$h\hat{\sigma}_\mu \hat{\sigma}_u + h^*\hat{\sigma}_u \hat{\sigma}_\mu = 2\epsilon_{\text{F}}\delta_{\mu u} - 2\eta\epsilon_{\mu u \nu}\hat{\sigma}_\nu. \tag{B36}$$

As a result, $\hat{I}^{(2)}_{\mu\xi}$ is obtained by

$$\hat{I}^{(2)}_{\mu(=x,y)\xi} = \frac{\hbar\tilde{v}_F i \pi \nu_e}{8\eta^2}\epsilon_{\xi zu}\left[\left(1+2\frac{\eta^2}{\epsilon_F^2}\right)\delta_{\mu u}+\frac{\eta}{\epsilon_F}\epsilon_{\mu u\nu}\hat{\sigma}_\nu\right]+O\left(\frac{\hbar}{\epsilon_F\tau}\right)=\frac{i\pi\nu_e}{8\eta^2}\hbar\tilde{v}_F\epsilon_{\mu\xi z}+O\left(\frac{\hbar}{\epsilon_F\tau}\right),\tag{B37}$$

$$\hat{I}^{(2)}_{z\xi} = \frac{\hbar\tilde{v}_F i \pi \nu_e}{8\eta^2}\epsilon_{\xi zu}\left[\left(1+2\frac{\eta^2}{\epsilon_F^2}\right)\delta_{zu}+\frac{\eta}{\epsilon_F}\epsilon_{zu\nu}\hat{\sigma}_\nu\right]+O\left(\frac{\hbar}{\epsilon_F\tau}\right)=\frac{i\pi\nu_e}{8\epsilon_F\eta}\hbar\tilde{\xi}_F+O\left(\frac{\hbar}{\epsilon_F\tau}\right).\tag{B38}$$

4. Calculation of $\hat{I}^{(3)}_{\mu(=x,y,z)\xi\xi'}$

$\hat{I}^{(3)}_{\mu\xi\xi'}$ in Eq. (B5) is represented by using the partial integral as

$$\hat{I}^{(3)}_{\mu\xi\xi'} = \frac{1}{4}\sum_{\boldsymbol{k}}\left[\frac{\partial^2\hat{g}^{\mathrm{r}}_{\boldsymbol{k}}}{\partial k_\xi\partial k_{\xi'}}\hat{\sigma}_\mu\hat{g}^{\mathrm{a}}_{\boldsymbol{k}}+\mathrm{H.c.}\right].\tag{B39}$$

In order to consider $\langle\frac{\partial^2\hat{g}^{\mathrm{r}}_{\boldsymbol{k}}}{\partial k_\xi\partial k_{\xi'}}\hat{\sigma}_\mu\hat{g}^{\mathrm{a}}_{\boldsymbol{k}}\rangle_k$, we use the following equations:

$$\frac{\partial D^{\mathrm{r}}}{\partial k_{\xi'}} = 2\hbar^2\tilde{v}_F^2 k'_\xi(D^{\mathrm{r}})^2,\tag{B40}$$

$$\frac{\partial\hat{Q}(D^{\mathrm{r}})^2}{\partial k_{\xi'}} = \hbar\tilde{v}_F(z\times\hat{\boldsymbol{\sigma}})_{\xi'}(D^{\mathrm{r}})^2+4\hbar^2\tilde{v}_F^2 k_{\xi'}\hat{Q}(D^{\mathrm{r}})^3,\tag{B41}$$

$$\frac{\partial^2\hat{g}^{\mathrm{r}}_{\boldsymbol{k}}}{\partial k_\xi\partial k_{\xi'}} = 2\hbar^2\tilde{v}_F^2\{\delta_{\xi\xi'}\hat{Q}(D^{\mathrm{r}})^2+4\hbar^2\tilde{v}_F^2 k_\xi k_{\xi'}\hat{Q}(D^{\mathrm{r}})^3+\hbar\tilde{v}_F[k_\xi(z\times\hat{\boldsymbol{\sigma}})_{\xi'}+k_{\xi'}(z\times\hat{\boldsymbol{\sigma}})_\xi](D^{\mathrm{r}})^2\},\tag{B42}$$

$$\frac{\partial^2\hat{g}^{\mathrm{r}}_{\boldsymbol{k}}}{\partial k_\xi\partial k_{\xi'}}\hat{\sigma}_\mu\hat{g}^{\mathrm{a}}_{\boldsymbol{k}} = 2\hbar^2\tilde{v}_F^2\{\delta_{\xi\xi'}\hat{Q}(D^{\mathrm{r}})^2\hat{\sigma}_\mu\hat{Q}^\dagger D^{\mathrm{a}}+4\hbar^2\tilde{v}_F^2 k_\xi k_{\xi'}\hat{Q}(D^{\mathrm{r}})^3\hat{\sigma}_\mu\hat{Q}^\dagger D^{\mathrm{a}}+\hbar\tilde{v}_F[k_\xi(z\times\hat{\boldsymbol{\sigma}})_{\xi'}+k_{\xi'}(z\times\hat{\boldsymbol{\sigma}})_\xi](D^{\mathrm{r}})^2\hat{\sigma}_\mu\hat{Q}^\dagger D^{\mathrm{a}}\}.\tag{B43}$$

The averages of $\boldsymbol{k}$ in $\hat{Q}\hat{\sigma}_\mu\hat{Q}^\dagger$, $k_\xi(z\times\hat{\boldsymbol{\sigma}})_{\xi'}\hat{\sigma}_\mu\hat{Q}^\dagger$, and $k_\xi k_{\xi'}\hat{Q}\hat{\sigma}_\mu\hat{Q}^\dagger$ become

$$\langle\hat{Q}\hat{\sigma}_\mu\hat{Q}^\dagger\rangle_k = |h|^2\hat{\sigma}_\mu-\hbar^2\tilde{v}_F^2 k^2\delta_{\mu z}\hat{\sigma}_z,\tag{B44}$$

$$\langle k_\xi(z\times\hat{\boldsymbol{\sigma}})_{\xi'}\hat{\sigma}_\mu\hat{Q}^\dagger\rangle_k = \tfrac{1}{2}\hbar\tilde{v}_F k^2(z\times\hat{\boldsymbol{\sigma}})_{\xi'}\hat{\sigma}_\mu(z\times\hat{\boldsymbol{\sigma}})_\xi,\tag{B45}$$

$$\langle k_\xi k_{\xi'}\hat{Q}\hat{\sigma}_\mu\hat{Q}^\dagger\rangle_k = |h|^2\langle k_\xi k_{\xi'}\rangle_k\hat{\sigma}_\mu+\hbar^2\tilde{v}_F^2\langle k_\xi k_{\xi'}k_\ell k_{\ell'}\rangle_k(z\times\hat{\boldsymbol{\sigma}})_\ell\hat{\sigma}_\mu(z\times\hat{\boldsymbol{\sigma}})_{\ell'}.\tag{B46}$$

Here, we have used $\langle k_\xi k_{\xi'}k_\ell k_{\ell'}\rangle_k = \frac{k^4}{8}(\delta_{\xi\xi'}\delta_{\ell\ell'}+\delta_{\xi\ell}\delta_{\xi'\ell'}+\delta_{\xi\ell'}\delta_{\xi'\ell})$. Then, $\hat{I}^{(3)}_{\mu\xi\xi'}$ is given by

$$\hat{I}^{(3)}_{\mu(=x,y)\xi\xi'} = \frac{\hbar^2\tilde{v}_F^2}{2}\sum_{\boldsymbol{k}}\left\{\left[\delta_{\xi\xi'}\hat{\sigma}_\mu|h|^2(D^{\mathrm{r}})^2 D^{\mathrm{a}}+\frac{1}{2}\hbar^2\tilde{v}_F^2 k^2(D^{\mathrm{r}})^2 D^{\mathrm{a}}[(z\times\hat{\boldsymbol{\sigma}})_{\xi'}\hat{\sigma}_\mu(z\times\hat{\boldsymbol{\sigma}})_\xi+(\xi\leftrightarrow\xi')]+2|h|^2\hbar^2\tilde{v}_F^2 k^2\delta_{\xi\xi'}\hat{\sigma}_\mu(D^{\mathrm{r}})^3 D^{\mathrm{a}}\right.\right.$$

$$\left.\left.+\frac{1}{2}\hbar^4\tilde{v}_F^4 k^4(D^{\mathrm{r}})^3 D^{\mathrm{a}}[(z\times\hat{\boldsymbol{\sigma}})_\xi\hat{\sigma}_\mu(z\times\hat{\boldsymbol{\sigma}})_{\xi'}+(\xi\leftrightarrow\xi')]\right]+\mathrm{H.c.}\right\}\tag{B47}$$

$$= \frac{\hbar^2\tilde{v}_F^2}{2}\sum_{\boldsymbol{k}}\left[|h|^2\delta_{\xi\xi'}\hat{\sigma}_\mu\left(|D^{\mathrm{r}}|^2(D^{\mathrm{r}}+D^{\mathrm{a}})+2\hbar^2\tilde{v}_F^2 k^2|D^{\mathrm{r}}|^2\{(D^{\mathrm{r}})^2+(D^{\mathrm{a}})^2\}\right)\right.$$

$$\left.+\left[\hbar^2\tilde{v}_F^2 k^2|D^{\mathrm{r}}|^2(D^{\mathrm{r}}+D^{\mathrm{a}})+\hbar^4\tilde{v}_F^4 k^4|D^{\mathrm{r}}|^2\{(D^{\mathrm{r}})^2+(D^{\mathrm{a}})^2\}\right][\epsilon_{\xi z\mu}(z\times\hat{\boldsymbol{\sigma}})_{\xi'}+\epsilon_{\xi'z\mu}(z\times\hat{\boldsymbol{\sigma}})_\xi-\delta_{\xi\xi'}\hat{\sigma}_\mu]\right],\tag{B48}$$

$$\hat{I}^{(3)}_{z\xi\xi'} = \frac{\hbar^2\tilde{v}_F^2}{2}\delta_{\xi\xi'}\sum_{\boldsymbol{k}}\left\{\left[(|h|^2-2\hbar^2\tilde{v}_F^2 k^2)\hat{\sigma}_z(D^{\mathrm{r}})^2 D^{\mathrm{a}}+2(|h|^2\hbar^2\tilde{v}_F^2 k^2-\hbar^4\tilde{v}_F^4 k^4)(D^{\mathrm{r}})^3 D^{\mathrm{a}}\right]+\mathrm{H.c.}\right\},$$

Here, we have used

$$(z\times\hat{\boldsymbol{\sigma}})_\xi\hat{\sigma}_\mu(z\times\hat{\boldsymbol{\sigma}})_{\xi'}+(\xi\leftrightarrow\xi')=2[\epsilon_{\xi z\mu}(z\times\hat{\boldsymbol{\sigma}})_{\xi'}+\epsilon_{\xi'z\mu}(z\times\hat{\boldsymbol{\sigma}})_\xi-\delta_{\xi\xi'}\hat{\sigma}_\mu].$$

$\hat{I}^{(3)}_{\mu\xi\xi'}$ is given by using equations in Appendix F as

$$\hat{I}^{(3)}_{\mu(=x,y)\xi\xi'} = -\hbar^2\tilde{v}_F^2\frac{\pi\nu_e}{64\eta^3}[\epsilon_{\xi z\mu}\epsilon_{\xi'z\nu}+\epsilon_{\xi'z\mu}\epsilon_{\xi z\nu}+\delta_{\xi\xi'}\delta_{\nu\mu}]\hat{\sigma}_\nu+O\left(\frac{\hbar}{\epsilon_F\tau}\right),\tag{B49}$$

$$\hat{I}^{(3)}_{z\xi\xi'} = \hbar^2\tilde{v}_F^2\frac{\pi\nu_e}{8\epsilon_F^2\eta}+O\left(\frac{\hbar}{\epsilon_F\tau}\right).\tag{B50}$$

Using $q_\alpha q_\beta[\epsilon_{\alpha z\mu}\epsilon_{\beta z\nu} + \epsilon_{\beta z\mu}\epsilon_{\alpha z\nu} + \delta_{\alpha\beta}\delta_{\nu\mu}] = q_\alpha q_\beta[3\delta_{\alpha\beta}\delta_{\nu\mu} - 2\delta_{\alpha\nu}\delta_{\beta\mu}]$, we obtain

$$q_\alpha q_\beta \hat{I}^{(3)}_{\mu\alpha\beta} = -\hbar^2 \tilde{v}_F^2 \frac{\pi \nu_e}{64\eta^3} q_\alpha q_\beta [3\delta_{\alpha\beta}\delta_{\nu\mu} - 2\delta_{\alpha\nu}\delta_{\beta\mu}]\hat{\sigma}_\nu. \tag{B51}$$

Thus, $\hat{I}_\mu = \hat{I}^{(0)}_\mu + \Omega\hat{I}^{(1)}_\mu + q_\xi \hat{I}^{(2)}_{\mu\xi} + q_\xi q_{\xi'}\hat{I}^{(3)}_{\mu\xi\xi'}$ is obtained by

$$\hat{I}_{\mu=x,y} \simeq \frac{\pi \nu_e}{4\eta}\left[\left(1 - i\Omega\tau - \frac{3}{2}D\tau q^2\right)\hat{\sigma}_\mu + iq_\alpha \ell\epsilon_{\mu\alpha z} + D\tau q_\mu q_\nu \hat{\sigma}_\nu\right], \quad \hat{I}_{\mu=z} \simeq O\left(\frac{\hbar}{\epsilon_F \tau}\right), \tag{B52}$$

where $D = \frac{1}{2}\tilde{v}_F^2\tau$ and $\ell = \tilde{v}_F\tau$ are the diffusion constant and the mean-free path of the surface electrons, respectively.

APPENDIX C: CALCULATION OF $\hat{I}_0$

We will calculate $\hat{I}_0$ using the same formalism in the Appendix B. Here, $\hat{I}_0 = \sum_k \hat{g}^r_{k-\frac{q}{2},-\frac{\Omega}{2}} \hat{g}^a_{k+\frac{q}{2},\frac{\Omega}{2}}$ can be expanded with respect to q and Ω within $q\ell \ll 1$ and $\Omega\tau \ll 1$ as

$$\hat{I}_0 \equiv \hat{I}^{(0)}_0 + \Omega\hat{I}^{(1)}_0 + \sum_{\xi=x,y} q_\xi \hat{I}^{(2)}_{0\xi} + \sum_{\xi,\xi'=x,y} q_\xi q_{\xi'}\hat{I}^{(3)}_{0\xi\xi'}, \tag{C1}$$

$$\hat{I}^{(0)}_0 = \sum_k \hat{g}^r_k \hat{g}^a_k, \tag{C2}$$

$$\hat{I}^{(1)}_0 = \frac{1}{2}\sum_k\left(\hat{g}^r_k \frac{\partial \hat{g}^a_{k,\omega}}{\partial\omega}\bigg|_{\omega\to 0} - \text{H.c.}\right), \tag{C3}$$

$$\hat{I}^{(2)}_{0\xi} = \frac{1}{2}\sum_k\left(\hat{g}^r_k \frac{\partial \hat{g}^a_k}{\partial k_\xi} - \text{H.c.}\right), \tag{C4}$$

$$\hat{I}^{(3)}_{0\xi\xi'} = \frac{1}{8}\sum_k\left(\hat{g}^r_k \frac{\partial^2 \hat{g}^a_k}{\partial k_\xi \partial k_{\xi'}} + \frac{\partial^2 \hat{g}^r_k}{\partial k_\xi \partial k_{\xi'}}\hat{g}^a_k - 2\frac{\partial \hat{g}^r_k}{\partial k_\xi}\frac{\partial \hat{g}^a_k}{\partial k_{\xi'}}\right). \tag{C5}$$

1. Calculation of $\hat{I}^{(0)}_0$

We will calculate $\hat{I}^{(0)}_0$ in Eq. (C2). By using $\hat{g}^r_k \hat{g}^a_k = D^r D^a |\hat{\mathcal{Q}}|^2$ and $\langle\hat{\mathcal{Q}}\hat{\mathcal{Q}}^\dagger\rangle_k = [|h|^2 + \hbar^2\tilde{v}_F^2 k^2]$, $\hat{I}^{(0)}_0$ becomes

$$\hat{I}^{(0)}_0 = \sum_k |D^r|^2\left[|h|^2 + \hbar^2\tilde{v}_F^2 k^2\right]. \tag{C6}$$

The above equation can be estimated around the Fermi energy $k \to k_F \equiv \epsilon_F/(\hbar\tilde{v}_F)$ as

$$\hat{I}^{(0)}_0 \sim \left[|h|^2 + \hbar^2\tilde{v}_F^2 k_F^2\right]\sum_k |D^r|^2 = \frac{\pi\nu_e}{2\eta}. \tag{C7}$$

2. Calculation of $\hat{I}^{(1)}_0$

$\hat{I}^{(1)}_0$ in Eq. (C3) is calculated by using

$$\hat{g}^r_k \frac{\partial \hat{g}^a_{k,\omega}}{\partial\omega}\bigg|_{\omega\to 0} = -\hbar D^r (D^a)^2 \hat{\mathcal{Q}}(\hat{\mathcal{Q}}^\dagger)^2, \tag{C8}$$

$$|Q|^2 = \left\{|h|^2 + \hbar^2\tilde{v}_F^2 k^2\right\} + (h + h^*)\hbar\tilde{v}_F \boldsymbol{k}\cdot(\boldsymbol{z}\times\hat{\boldsymbol{\sigma}}), \tag{C9}$$

$$\langle\hat{\mathcal{Q}}(\hat{\mathcal{Q}}^\dagger)^2\rangle_k = |h|^2 h^* + (h + 2h^*)\hbar^2\tilde{v}_F^2 k^2, \tag{C10}$$

$$\langle\hat{\mathcal{Q}}^2\hat{\mathcal{Q}}^\dagger\rangle_k = |h|^2 h + (2h + h^*)\hbar^2\tilde{v}_F^2 k^2, \tag{C11}$$

$h + h^* = 2\epsilon_F$, and $h^* D^a - h D^r = \epsilon_F(D^a - D^r) - i\eta(D^a + D^r)$ as

$$\hat{I}^{(1)}_0 = -\frac{\hbar}{2}\sum_k\left[\epsilon_F\left(|h|^2 + \hbar^2\tilde{v}_F^2 k^2\right)|D^r|^2(D^a - D^r) - i\eta\left(|h|^2 + \hbar^2\tilde{v}_F^2 k^2\right)|D^r|^2(D^a + D^r) + 2\epsilon_F\hbar^2\tilde{v}_F^2 k^2|D^r|^2(D^a - D^r)\right]$$

$$= -\frac{i\pi\nu_e}{4\eta^2}\hbar + O\left(\frac{\hbar}{\epsilon_F\tau}\right). \tag{C12}$$

3. Calculation of $\hat{I}_{0\xi}^{(2)}$

$\hat{I}_{0\xi}^{(2)}$ in Eq. (C4) is obtained by

$$\hat{I}_{0\xi}^{(2)} = \frac{\hbar\tilde{v}_F}{2} \sum_k \epsilon_{\xi z\ell} \hat{\sigma}_\ell \big[(h - h^*) + 2\epsilon_F\hbar^2\tilde{v}_F^2 k^2 (D^a - D^r)\big] |D^r|^2 \simeq \frac{\pi\nu_e}{2\eta} \frac{i\tilde{v}_F\tau}{2} \epsilon_{\xi z\ell} \hat{\sigma}_\ell. \tag{C13}$$

Here, we have used the following equations:

$$\langle k_\xi |\hat{\mathcal{Q}}|^2 \rangle_k = \tfrac{1}{2}\hbar\tilde{v}_F(h + h^*)k^2(z \times \hat{\boldsymbol{\sigma}})_\xi = \epsilon_F\hbar\tilde{v}_F k^2 \epsilon_{\xi z\alpha}\hat{\sigma}_\alpha, \tag{C14}$$

$$\left\langle \frac{\partial\hat{g}_k^r}{\partial k_\xi} \hat{g}_k^a \right\rangle_k = \hbar\tilde{v}_F\epsilon_{\xi z\ell}\hat{\sigma}_\ell\big[h^* + 2\hbar^2\tilde{v}_F^2 k^2 \epsilon_F D^r\big]|D^r|^2. \tag{C15}$$

4. Calculation of $\hat{I}_{0\xi\xi'}^{(3)}$

$\frac{\partial\hat{g}^r}{\partial k_\alpha}\frac{\partial\hat{g}^a}{\partial k_\beta}$ becomes

$$\frac{1}{\hbar^2\tilde{v}_F^2}\frac{\partial\hat{g}^r}{\partial k_\alpha}\frac{\partial\hat{g}^a}{\partial k_\beta} = \epsilon_{\alpha z\ell}\epsilon_{\beta z\ell'}\hat{\sigma}_\ell\hat{\sigma}_{\ell'}|D^r|^2 + 4\hbar^2\tilde{v}_F^2 k_\alpha k_\beta|\hat{\mathcal{Q}}|^2|D^r|^4 + 2\hbar\tilde{v}_F\epsilon_{\alpha z\ell}\{\hat{\sigma}_\ell k_\beta\hat{\mathcal{Q}}^\dagger\}|D^r|^2 D^a + 2\hbar\tilde{v}_F\epsilon_{\beta z\ell'}\{k_\alpha\hat{\mathcal{Q}}\hat{\sigma}_{\ell'}\}|D^r|^2 D^r. \tag{C16}$$

The average $\langle \frac{\partial\hat{g}^r}{\partial k_\alpha}\frac{\partial\hat{g}^a}{\partial k_\beta} \rangle_k$ is reduced to be

$$\frac{1}{\hbar^2\tilde{v}_F^2}\left\langle \frac{\partial\hat{g}^r}{\partial k_\alpha}\frac{\partial\hat{g}^a}{\partial k_\beta} \right\rangle_k = \epsilon_{\alpha z\ell}\epsilon_{\beta z\ell'}\hat{\sigma}_\ell\hat{\sigma}_{\ell'}|D^r|^2 + 2\delta_{\alpha\beta}|h|^2(\hbar\tilde{v}_F k)^2|D^r|^4 + 2\delta_{\alpha\beta}(\hbar\tilde{v}_F k)^4|D^r|^4$$
$$+ \epsilon_{\alpha z\ell}\epsilon_{\beta uz}\hat{\sigma}_\ell\hat{\sigma}_u(\hbar\tilde{v}_F k)^2|D^r|^2 D^a + \epsilon_{\beta z\ell}\epsilon_{\alpha u'z}\hat{\sigma}_{u'}\hat{\sigma}_\ell(\hbar\tilde{v}_F k)^2|D^r|^2 D^r. \tag{C17}$$

After we integrate the above equation as a function of k, we obtain

$$\frac{q_\alpha q_\beta}{\hbar^2\tilde{v}_F^2}\sum_k \frac{\partial\hat{g}^r}{\partial k_\alpha}\frac{\partial\hat{g}^a}{\partial k_\beta} = \delta_{\alpha\beta}\sum_k\{|D^r|^2 + 2[|h|^2(\hbar\tilde{v}_F k)^2 + (\hbar\tilde{v}_F k)^4]|D^r|^4] - (\hbar\tilde{v}_F k)^2|D^r|^2(D^a + D^r)\}q_\alpha q_\beta = \frac{\pi\nu_e}{8\eta^3}q^2 + O\left(\frac{\hbar}{\epsilon_F\tau}\right). \tag{C18}$$

Here, we have used

$$q_\alpha q_\beta\epsilon_{\alpha z\ell}\delta_{\beta\ell} = 0, \tag{C19}$$

$$q_\alpha q_\beta\epsilon_{\alpha z\ell}\epsilon_{\beta z\ell'}\hat{\sigma}_\ell\hat{\sigma}_{\ell'} = q_\alpha q_\beta\delta_{\alpha\beta}, \tag{C20}$$

$$q_\alpha q_\beta\epsilon_{\alpha\ell z}\epsilon_{\beta uz}\epsilon_{\ell u\xi} = q_\alpha q_\beta(\delta_{\alpha\beta}\delta_{\ell u} - \delta_{\alpha u}\delta_{\beta\ell})\epsilon_{\ell u\xi} = 0, \tag{C21}$$

$$q_\alpha q_\beta\epsilon_{\alpha z\ell}\epsilon_{\beta uz}(\hat{\sigma}_\ell\hat{\sigma}_u D^a + \hat{\sigma}_u\hat{\sigma}_\ell D^r) = -q_\alpha q_\beta\delta_{\alpha\beta}(D^a + D^r). \tag{C22}$$

Thus, $q_\xi q_{\xi'} I_{0\xi\xi'}^{(3)}$ becomes

$$q_\xi q_{\xi'} I_{0\xi\xi'}^{(3)} = -\hbar^2\tilde{v}_F^2\frac{\pi\nu_e}{16\eta^3}q^2 + O\left(\frac{\hbar}{\epsilon_F\tau}\right). \tag{C23}$$

APPENDIX D: CALCULATION OF $\hat{\Gamma}_\nu^{rr}$

We estimate $\hat{\Gamma}_\nu^{rr} = n_i u_i^2 \sum_k \hat{g}_{k-\frac{q}{2},\omega-\frac{\Omega}{2}}^r \hat{\sigma}_\mu \hat{g}_{k+\frac{q}{2},\omega+\frac{\Omega}{2}}^r$ by using the same formalism in Appendixes B and C. Here, $\hat{\Gamma}_\nu^{rr} = n_i u_i^2 \sum_k \hat{g}_{k-\frac{q}{2},\omega-\frac{\Omega}{2}}^r \hat{\sigma}_\mu \hat{g}_{k+\frac{q}{2},\omega+\frac{\Omega}{2}}^r$ can be expanded as

$$n_i u_i^2 \sum_k \hat{g}_{k-\frac{q}{2},\omega-\frac{\Omega}{2}}^r \hat{\sigma}_\mu \hat{g}_{k+\frac{q}{2},\omega+\frac{\Omega}{2}}^r = \hat{C}_\mu^{rr(0)} + \Omega\hat{C}_\mu^{rr(1)} + \sum_{\xi=x,y} q_\xi\hat{C}_{\mu\xi}^{rr(2)} + \sum_{\xi,\xi'=x,y} q_\xi q_{\xi'}\hat{C}_{\mu\xi\xi'}^{rr(3)} + O(q^3, q\Omega, \Omega^2), \tag{D1}$$

where coefficients in the above equation are given by

$$\hat{C}_\mu^{rr(0)} = n_i u_i^2 \sum_k [\hat{g}^r \hat{\sigma}_\mu \hat{g}^r] = \begin{cases} -\frac{n_i u_i^2 \nu_e}{2\epsilon_F}\hat{\sigma}_\mu & (\mu = x, y), \\ -\frac{i n_i u_i^2 \pi\nu_e}{2\epsilon_F}\arg(-\hbar\omega - \epsilon_F + i\eta)\hat{\sigma}_z & (\mu = z), \\ -\frac{n_i u_i^2 \nu_e}{\epsilon_F} + \frac{i n_i u_i^2 \pi\nu_e}{2\epsilon_F}\arg(-\hbar\omega - \epsilon_F + i\eta) & (\mu = 0), \end{cases} \tag{D2}$$

$$\hat{C}_\mu^{\mathrm{rr}(1)} = \frac{n_\mathrm{i} u_\mathrm{i}^2}{2} \sum_{\bm{k}} \left[\hat{g}^\mathrm{r} \hat{\sigma}_\mu \frac{\partial \hat{g}^\mathrm{r}}{\partial \omega} - \frac{\partial \hat{g}^\mathrm{r}}{\partial \omega} \hat{\sigma}_\mu \hat{g}^\mathrm{r} \right] = 0, \tag{D3}$$

$$\hat{C}_{\mu\xi}^{\mathrm{rr}(2)} = \frac{n_\mathrm{i} u_\mathrm{i}^2}{2} \sum_{\bm{k}} \left[\hat{g}^\mathrm{r} \hat{\sigma}_\mu \frac{\partial \hat{g}^\mathrm{r}}{\partial k_\xi} - \frac{\partial \hat{g}^\mathrm{r}}{\partial k_\xi} \hat{\sigma}_\mu \hat{g}^\mathrm{r} \right] = \begin{cases} \frac{n_\mathrm{i} u_\mathrm{i}^2 \hbar v_F v_e}{2\epsilon_F[(\hbar\omega+\epsilon_F)^2+\eta^2]} [i(\hbar\omega + \epsilon_\mathrm{F}) + \eta] \delta_{\xi\mu} \hat{\sigma}_z & (\mu = x, y), \\ -\frac{n_\mathrm{i} u_\mathrm{i}^2 \hbar v_F v_e}{2\epsilon_F[(\hbar\omega+\epsilon_F)^2+\eta^2]} [i(\hbar\omega + \epsilon_\mathrm{F}) + \eta] \hat{\sigma}_\xi & (\mu = z), \\ 0 & (\mu = 0), \end{cases} \tag{D4}$$

$$\hat{C}_{\mu\xi\xi'}^{\mathrm{rr}(3)} = \frac{n_\mathrm{i} u_\mathrm{i}^2}{4} \sum_{\bm{k}} \left[\hat{g}^\mathrm{r} \hat{\sigma}_\mu \frac{\partial^2 \hat{g}^\mathrm{r}}{\partial k_\xi \partial k_{\xi'}} + \frac{\partial^2 \hat{g}^\mathrm{r}}{\partial k_\xi \partial k_{\xi'}} \hat{\sigma}_\mu \hat{g}^\mathrm{r} \right]$$

$$= \begin{cases} \frac{n_\mathrm{i} u_\mathrm{i}^2 \hbar^2 v_F^2 v_e}{12\epsilon_F[(\hbar\omega+\epsilon_F)^2+\eta^2]^2} [(\hbar\omega + \epsilon_\mathrm{F})^2 - \eta^2 - 2i\eta(\hbar\omega + \epsilon_\mathrm{F})][\epsilon_{\xi z \mu}(\bm{z} \times \hat{\bm{\sigma}})_{\xi'} + \epsilon_{\xi' z \mu}(\bm{z} \times \hat{\bm{\sigma}})_\xi - 2\delta_{\xi\xi'}\hat{\sigma}_\mu] & (\mu = x, y), \\ -\frac{n_\mathrm{i} u_\mathrm{i}^2 \hbar^2 v_F^2 v_e}{4\epsilon_F[(\hbar\omega+\epsilon_F)^2+\eta^2]^2} [(\hbar\omega + \epsilon_\mathrm{F})^2 - \eta^2 - 2i\eta(\hbar\omega + \epsilon_\mathrm{F})]\delta_{\xi\xi'}\hat{\sigma}_z & (\mu = z), \\ \frac{n_\mathrm{i} u_\mathrm{i}^2 \hbar^2 v_F^2 v_e}{12\epsilon_F[(\hbar\omega+\epsilon_F)^2+\eta^2]^2} [(\hbar\omega + \epsilon_\mathrm{F})^2 - \eta^2 - 2i\eta(\hbar\omega + \epsilon_\mathrm{F})]\delta_{\xi\xi'} & (\mu = 0). \end{cases} \tag{D5}$$

From Eqs. (D2)–(D5) and $n_\mathrm{i} u_\mathrm{i}^2 \pi v_e / \eta = 2$, the elements of $\hat{\Gamma}_\nu^{\mathrm{rr}}$ are negligibly small as compared with those of $\hat{\Gamma}_\nu^{\mathrm{ra}}$ since $\frac{\hbar}{\epsilon_\mathrm{F} \tau} \ll 1$ is satisfied.

APPENDIX E: CALCULATION OF $\hat{\Pi}_\nu^{\mathrm{rr}} + \hat{\Pi}_\nu^{\mathrm{aa}}$ ($\nu = x, y$)

We estimate the response function composed of only the retarded (advanced) Green's functions $\hat{\Pi}_\nu^{\mathrm{rr}}(\bm{q}, \Omega)$ [$\hat{\Pi}_\nu^{\mathrm{aa}}(\bm{q}, \Omega)$] using the same formalism in Appendixes B, C, and D. From Eqs. (22) and (23), $\hat{\Pi}_\nu^{\mathrm{rr}}(\bm{q}, \Omega) + \hat{\Pi}_\nu^{\mathrm{aa}}(\bm{q}, \Omega)$ are written as

$$\hat{\Pi}_\nu^{\mathrm{rr}}(\bm{q}, \Omega) + \hat{\Pi}_\nu^{\mathrm{aa}}(\bm{q}, \Omega) = -\sum_{\bm{k},\omega} \left\{ f_\omega \left[\hat{g}_{\bm{k}-\frac{\bm{q}}{2},\omega-\frac{\Omega}{2}}^\mathrm{r} \hat{\sigma}_\nu \hat{g}_{\bm{k}+\frac{\bm{q}}{2},\omega+\frac{\Omega}{2}}^\mathrm{r} - \left(\hat{g}_{\bm{k}+\frac{\bm{q}}{2},\omega+\frac{\Omega}{2}}^\mathrm{r} \hat{\sigma}_\nu \hat{g}_{\bm{k}-\frac{\bm{q}}{2},\omega-\frac{\Omega}{2}}^\mathrm{r} \right)^\dagger \right] \right.$$
$$\left. + \frac{1}{2} \Omega f'_\omega \left[\hat{g}_{\bm{k}-\frac{\bm{q}}{2},\omega-\frac{\Omega}{2}}^\mathrm{r} \hat{\sigma}_\nu \hat{g}_{\bm{k}+\frac{\bm{q}}{2},\omega+\frac{\Omega}{2}}^\mathrm{r} + \left(\hat{g}_{\bm{k}+\frac{\bm{q}}{2},\omega+\frac{\Omega}{2}}^\mathrm{r} \hat{\sigma}_\nu \hat{g}_{\bm{k}-\frac{\bm{q}}{2},\omega-\frac{\Omega}{2}}^\mathrm{r} \right)^\dagger \right] \right\}. \tag{E1}$$

The magnitude of second term of the above equation is smaller than that of $\hat{\Pi}_\nu^{\mathrm{ra}}$ [see Eqs. (21) and Appendixes B, C, and D]. The first term is expanded as

$$-\sum_{\bm{k},\omega} f_\omega \left[\hat{g}_{\bm{k}-\frac{\bm{q}}{2},\omega-\frac{\Omega}{2}}^\mathrm{r} \hat{\sigma}_\nu \hat{g}_{\bm{k}+\frac{\bm{q}}{2},\omega+\frac{\Omega}{2}}^\mathrm{r} - \left(\hat{g}_{\bm{k}+\frac{\bm{q}}{2},\omega+\frac{\Omega}{2}}^\mathrm{r} \hat{\sigma}_\nu \hat{g}_{\bm{k}-\frac{\bm{q}}{2},\omega-\frac{\Omega}{2}}^\mathrm{r} \right)^\dagger \right] = \hat{D}_\nu^{(0)} + \Omega \hat{D}_\nu^{(1)} + \sum_{\xi=x,y} q_\xi \hat{D}_{\nu\xi}^{(2)} + O(q^2, q\Omega, \Omega^2), \tag{E2}$$

where $\hat{D}_\nu^{(0)}$, $\hat{D}_\nu^{(1)}$, and $\hat{D}_{\nu\xi}^{(2)}$ in the above equation are given by

$$\hat{D}_\nu^{(0)} = -\sum_{\bm{k},\omega} f_\omega \left[\hat{g}_{\bm{k},\omega}^\mathrm{r} \hat{\sigma}_\nu \hat{g}_{\bm{k},\omega}^\mathrm{r} - \mathrm{H.c.} \right] = 0, \tag{E3}$$

$$\hat{D}_\nu^{(1)} = -\frac{1}{2} \sum_{\bm{k},\omega} f_\omega \left[\left(\hat{g}_{\bm{k},\omega}^\mathrm{r} \hat{\sigma}_\mu \frac{\partial \hat{g}_{\bm{k},\omega}^\mathrm{r}}{\partial \omega} - \frac{\partial \hat{g}_{\bm{k},\omega}^\mathrm{r}}{\partial \omega} \hat{\sigma}_\mu \hat{g}_{\bm{k},\omega}^\mathrm{r} \right) + \mathrm{H.c.} \right] = 0, \tag{E4}$$

$$\hat{D}_{\nu\xi}^{(2)} = -\frac{1}{2} \sum_{\bm{k},\omega} f_\omega \left[\left(\hat{g}_{\bm{k},\omega}^\mathrm{r} \hat{\sigma}_\mu \frac{\partial \hat{g}_{\bm{k},\omega}^\mathrm{r}}{\partial k_\xi} - \frac{\partial \hat{g}_{\bm{k},\omega}^\mathrm{r}}{\partial k_\xi} \hat{\sigma}_\mu \hat{g}_{\bm{k},\omega}^\mathrm{r} \right) + \mathrm{H.c.} \right] = -\frac{\pi \tilde{v}_\mathrm{F} v_\mathrm{e}}{2\epsilon_\mathrm{F}} \hat{\sigma}_z + O\left(\frac{\hbar}{\epsilon_\mathrm{F} \tau} \right). \tag{E5}$$

Here, we have used $f_\omega = \theta(-\omega)$ in the above equation, where $\theta(x)$ is a step function. From Eqs. (9), (14), (47), and (E5), there are spin density and charge current induced by the magnetic field ($i\bm{q} \times \bm{A}_\mathrm{em}$). Since we consider only the electric field, we ignore the densities induced by the magnetic field.

We find that the order of $(\hat{\Pi}_\nu^{\mathrm{rr}} + \hat{\Pi}_\nu^{\mathrm{aa}}) / \hat{\Pi}_\nu^{\mathrm{ra}}$ is $\hbar/\epsilon_\mathrm{F}\tau$ and $\hat{\Pi}_\nu^{\mathrm{rr}} + \hat{\Pi}_\nu^{\mathrm{aa}}$ is negligibly small as compared with $\hat{\Pi}_\nu^{\mathrm{ra}}$.

APPENDIX F: CALCULATION OF INTEGRAL

We will show the following integrals as a functions of $\bm{k}$. The integrals are obtained by

$$\sum_{\bm{k}} D^\mathrm{r}(D^\mathrm{a})^2 \simeq \frac{v_e}{16\eta^2 \epsilon_\mathrm{F}^3} \left(i\pi - \frac{4\eta^2}{\epsilon_\mathrm{F}^2} \right), \tag{F1}$$

$$\sum_{\bm{k}} \hbar^2 \tilde{v}_\mathrm{F}^2 k^2 D^\mathrm{r}(D^\mathrm{a})^2 \simeq \frac{i\pi v_e}{16\eta^2 \epsilon_\mathrm{F}} \left(1 + i\frac{2\eta}{\epsilon_\mathrm{F}} \right), \tag{F2}$$

$$\sum_{\bm{k}} \left[(h^*)^2 + \hbar^2 \tilde{v}_\mathrm{F}^2 k^2 \right] D^\mathrm{r}(D^\mathrm{a})^2 \simeq \frac{v_e}{8\eta^2 \epsilon_\mathrm{F}} \left[i\pi - \frac{2\eta^2}{\epsilon_\mathrm{F}^2} \right], \tag{F3}$$

$$\sum_k \left[h(h^*)^2 + (h - 2h^*) \hbar^2 \tilde{v}_F^2 k^2 \right] D^r (D^a)^2 \simeq \frac{-i\pi \nu_e}{4\epsilon_F^2} \left(1 + i \frac{\eta}{\epsilon_F} \right), \tag{F4}$$

$$\sum_k \hbar^2 \tilde{v}_F^2 k^2 |D^r|^2 (D^a - D^r) \simeq \frac{i\pi \nu_e}{8\eta^2 \epsilon_F}, \tag{F5}$$

$$\sum_k |D^r|^2 \simeq \frac{\pi \nu_e}{4\eta \epsilon_F^2}, \tag{F6}$$

$$\sum_k [(D^r)^2 D^a + (D^a)^2 D^r] \simeq -\frac{\nu_e}{2\epsilon_F^5}, \tag{F7}$$

$$\sum_k (\hbar \tilde{v}_F k)^2 [(D^r)^2 D^a + (D^a)^2 D^r] \simeq -\frac{\pi \nu_e}{4\eta \epsilon_F^2}, \tag{F8}$$

$$\sum_k (\hbar \tilde{v}_F k)^2 (D^r)^3 D^a \simeq -\frac{\pi \nu_e}{64\epsilon_F^2 \eta^3} \left(1 - i \frac{2\eta}{\epsilon_F} \right), \tag{F9}$$

$$\sum_k (\hbar \tilde{v}_F k)^2 \{ (D^r)^3 D^a + (D^a)^3 D^r \} \simeq -\frac{\pi \nu_e}{32\epsilon_F^2 \eta^3}, \tag{F10}$$

$$\sum_k (\hbar \tilde{v}_F k)^4 (D^r)^3 D^a \simeq -\frac{\pi \nu_e}{32\eta^3}, \tag{F11}$$

$$\sum_k (\hbar v_F k)^2 (D^r)^n \simeq -\frac{1}{n-1} \sum_k (D^r)^{n-1} \quad (n \geqslant 3), \tag{F12}$$

$$\sum_k (\hbar v_F k)^4 (D^r)^n = \frac{2}{(n-1)(n-2)} \sum_k (D^r)^{n-2} \quad (n \geqslant 4), \tag{F13}$$

$$\sum_k (\hbar v_F k)^2 (D^r)^3 \simeq -\frac{1}{2} \sum_k (D^r)^2, \tag{F14}$$

$$\sum_k (\hbar v_F k)^2 (D^r)^4 \simeq -\frac{1}{3} \sum_k (D^r)^3 = \frac{\pi \nu_e}{32\epsilon_F^2 \eta^3}, \tag{F15}$$

$$\sum_k (\hbar v_F k)^4 (D^r)^4 \simeq \frac{1}{3} \sum_k (D^r)^2 = \frac{\pi \nu_e}{32\eta^3}, \tag{F16}$$

where $\sum_k$ is defined by

$$\sum_k \equiv \frac{1}{(2\pi)^2} \int_0^{2\pi} d\theta \int_0^\infty k \, dk = \frac{\nu_e}{2\pi \epsilon_F} \int_0^{2\pi} d\theta \int_0^\infty \epsilon \, d\epsilon = \frac{\nu_e}{4\pi \epsilon_F} \int_0^{2\pi} d\theta \int_0^\infty dx. \tag{F17}$$

Here, we have used $(D^r)^n = \frac{1}{2(n-1)\hbar^2 v_F^2 k_\xi} \frac{\partial (D^r)^{n-1}}{\partial k_\xi}$ in the above equation.

APPENDIX G: CHARGE CONSERVATION

To check the validity of our results, we substitute the charge current and charge density in Eqs. (48) and (39) into the charge conservation law $\dot{\rho}_e + \nabla \cdot \boldsymbol{j} = 0$. From Eq. (38), $\dot{\rho}_e$ becomes

$$\dot{\rho}_e = \frac{e^2 \tilde{v}_F^2 \ell \nu_e}{L^2} \sum_{\boldsymbol{q},\Omega} e^{i[\Omega t - \boldsymbol{q} \cdot \boldsymbol{x}]} \frac{i\Omega^2 q_\nu}{q^2 \ell^2 + i\Omega \tau} A_{\mathrm{em},\nu}. \tag{G1}$$

From Eqs. (36), (37), and $\boldsymbol{j} = 2e\tilde{v}_F (\boldsymbol{z} \times \boldsymbol{s})$, $\nabla \cdot \boldsymbol{j}$ becomes

$$\nabla_x j_x = \frac{e^2 \tilde{v}_F^2 \nu_e \tau}{L^2} \sum_{\boldsymbol{q},\Omega} e^{i[\Omega t - \boldsymbol{q} \cdot \boldsymbol{x}]} \left[-\Omega q_x A_{\mathrm{em},x} + \left\{ \frac{\Omega q_x^2 q_y \ell^2}{q^2 \ell^2 + i\Omega \tau} A_{\mathrm{em},y} + \frac{\Omega q_x^3 \ell^2}{q^2 \ell^2 + i\Omega \tau} A_{\mathrm{em},x} \right\} \right], \tag{G2}$$

$$\nabla_y j_y = \frac{e^2 \tilde{v}_F^2 \nu_e \tau}{L^2} \sum_{\boldsymbol{q},\Omega} e^{i[\Omega t - \boldsymbol{q} \cdot \boldsymbol{x}]} \left[-\Omega q_y A_{\mathrm{em},y} + \left\{ \frac{\Omega q_x q_y^2 \ell^2}{q^2 \ell^2 + i\Omega \tau} A_{\mathrm{em},x} + \frac{\Omega q_y^3 \ell^2}{q^2 \ell^2 + i\Omega \tau} A_{\mathrm{em},y} \right\} \right], \tag{G3}$$

$$\nabla_x j_x + \nabla_y j_y = -\frac{e^2 \tilde{v}_F^2 \ell \nu_e}{L^2} \sum_{\boldsymbol{q},\Omega} e^{i[\Omega t - \boldsymbol{q} \cdot \boldsymbol{x}]} \frac{i\Omega^2 q_\nu}{q^2 \ell^2 + i\Omega \tau} A_{\mathrm{em},\nu}. \tag{G4}$$

Therefore, ρ_e and $\boldsymbol{j}$ follow the charge conservation law $\dot{\rho}_e + \nabla \cdot \boldsymbol{j} = 0$.

APPENDIX H: DIFFUSIVE GREEN'S FUNCTION $\mathcal{D}$

The diffusive Green's function on the disordered surface of the TI can be integrated as follows:

$$\sum_{\Omega} \frac{e^{i(\Omega t - \boldsymbol{q} \cdot \boldsymbol{x})}}{i\Omega + 2Dq^2} \sim \frac{1}{2\pi i} \int_{-\infty}^{\infty} \frac{d\Omega}{\Omega - i2Dq^2} = \theta(t) \exp\left[-2Dtq^2 - i\boldsymbol{q} \cdot \boldsymbol{x}\right], \tag{H1}$$

$$\sum_{q_x} e^{-(2Dtq_x^2 + iq_x x)} \sim \frac{1}{2\pi} \int_{-\infty}^{\infty} dq_x e^{-(2Dtq_x^2 + iq_x x)} = \frac{\sqrt{\pi}}{2\pi\sqrt{2Dt}} \exp\left(-\frac{2x^2}{Dt}\right). \tag{H2}$$

Thus, from the above equations, $\mathcal{D}$ in the coordinate space is obtained by

$$\mathcal{D}(\boldsymbol{x}, t) \sim \frac{\theta(t)}{8\pi Dt} \exp\left[-\frac{1}{8Dt}(x^2 + y^2)\right]. \tag{H3}$$

[1] A. V. Kimel, A. Kirilyuk, P. A. Usachev, R. V. Pisarev, A. M. Balbashov, and Th. Rasing, Nature (London) **435**, 655 (2005).

[2] F. Hansteen, A. Kimel, A. Kirilyuk, and Th. Rasing, Phys. Rev. Lett. **95**, 047402 (2005).

[3] R. Iida, T. Satoh, T. Shimura, K. Kuroda, B. A. Ivanov, Y. Tokunaga, and Y. Tokura, Phys. Rev. B **84**, 064402 (2011).

[4] A. Kirilyuk, A. V. Kimel, and T. Rasing, Rev. Mod. Phys. **82**, 2731 (2010).

[5] C. D. Stanciu, F. Hansteen, A. V. Kimel, A. Kirilyuk, A. Tsukamoto, A. Itoh, and T. Rasing, Phys. Rev. Lett. **99**, 047601 (2007).

[6] K. Vahaplar, A. M. Kalashnikova, A. V. Kimel, D. Hinzke, U. Nowak, R. Chantrell, A. Tsukamoto, A. Itoh, A. Kirilyuk, and Th. Rasing, Phys. Rev. Lett. **103**, 117201 (2009).

[7] S. Raghu, S. B. Chung, X.-L. Qi, and S.-C. Zhang, Phys. Rev. Lett. **104**, 116401 (2010).

[8] T. Misawa, T. Yokoyama, and S. Murakami, Phys. Rev. B **84**, 165407 (2011).

[9] X. Liu and J. Sinova, Phys. Rev. Lett. **111**, 166801 (2013).

[10] M. Z. Hasan and C. L. Kane, Rev. Mod. Phys. **82**, 3045 (2010).

[11] X.-L. Qi and S.-C. Zhang, Rev. Mod. Phys. **83**, 1057 (2011).

[12] Y. Ando, J. Phys. Soc. Jpn. **82**, 102001 (2013).

[13] W. K. Tse and A. H. MacDonald, Phys. Rev. Lett. **105**, 057401 (2010).

[14] W. K. Tse and A. H. MacDonald, Phys. Rev. B **82**, 161104(R) (2010).

[15] G. F. Quinteiro and P. I. Tamborenea, Phys. Rev. B **79**, 155450 (2009).

[16] G. F. Quinteiro and P. I. Tamborenea, Phys. Rev. B **82**, 125207 (2010).

[17] G. F. Quinteiro, P. I. Tamborenea, and J. Berakdar, Opt. Express **19**, 26733 (2011).

[18] J. Wätzel, A. S. Moskalenko, and J. Berakdar, Opt. Express **20**, 27792 (2012).

[19] M. B. Farías, G. F. Quinteiro, and P. I. Tamborenea, Eur. Phys. J. B **86**, 432 (2013).

[20] M. Cygorek, P. I. Tamborenea, and V. M. Axt, Phys. Rev. B **92**, 115301 (2015).

[21] Y. Ueno, Y. Toda, S. Adachi, R. Morita, and T. Tawara, Opt. Express **17**, 20567 (2009).

[22] N. B. Clayburn, J. L. McCarter, J. M. Dreiling, M. Poelker, D. M. Ryan, and T. J. Gay, Phys. Rev. B **87**, 035204 (2013).

[23] L. Marrucci, C. Manzo, and D. Paparo, Phys. Rev. Lett. **96**, 163905 (2006).

[24] L. Allen, M. W. Beijersbergen, R. J. C. Spreeuw, and J. P. Woerdman, Phys. Rev. A **45**, 8185 (1992).

[25] G. Molina-Terriza, J. P. Torres, and L. Torner, Nat. Phys. **3**, 305 (2007).

[26] M. Padgett, J. Courtial, and L. Allen, Phys. Today **57**(5), 35 (2004).

[27] J. T. Mendonca, B. Thide, and H. Then, Phys. Rev. Lett. **102**, 185005 (2009).

[28] V. E. Lembessis, M. Babiker, and D. L. Andrews, Phys. Rev. A **79**, 011806(R) (2009).

[29] A. A. Taskin, S. Sasaki, K. Segawa, and Y. Ando, Phys. Rev. Lett. **109**, 066803 (2012).

[30] J. Fujimoto, A. Sakai, and H. Kohno, Phys. Rev. B **87**, 085437 (2013).

[31] A. Sakai and H. Kohno, Phys. Rev. B **89**, 165307 (2014).

[32] A. A. Burkov and D. G. Hawthorn, Phys. Rev. Lett. **105**, 066802 (2010).

[33] H. Haug and A. P. Jauho, *Quantum Kinetics in Transport and Optics of Semiconductors*, 2nd ed. (Springer, New York, 2007), pp. 45–46.

[34] J. Linder, T. Yokoyama, and A. Sudbo, Phys. Rev. B **80**, 205401 (2009).

[35] J. He, X. Wang, D. Hu, J. Ye, S. Feng, Q. Kan, and Y. Zhang, Opt. Express **21**, 20230 (2013).

[36] G. D. Mahan, *Many-Particle Physics*, 3rd ed. (Springer, New York, 2000), p. 514.

[37] K. Taguchi, K. Shintani, and Y. Tanaka, Phys. Rev. B **92**, 035425 (2015).

[38] Using $\frac{\hbar}{2\tau} = \frac{1}{2}\pi\nu_e n_i u_0^2$, $\nu_e = \frac{\epsilon_F}{2\pi\hbar^2 \tilde{v}_F^2}$, and $\tilde{v}_F/v_F = (1+\xi)^{-1}$, we can obtain the relation $\xi(1+\xi)^2 = \frac{\hbar}{4\pi\epsilon_F\tau}$. Because of $\frac{\hbar}{\epsilon_F\tau} \ll 1$, $\xi < \frac{\hbar}{2\pi\epsilon_F\tau}$ becomes negligibly small as $\tilde{v}_F/v_F = 1 + O(\frac{\hbar}{\epsilon_F\tau})$. Streakily speaking, there is no problem to take $\tilde{v}_F \simeq v_F$.

[39] V. M. Edelstein, Solid State Commun. **73**, 233 (1990).

[40] P. Schwab, R. Raimondi, and C. Gorini, Europhys. Lett. **93**, 67004 (2011).

[41] K. Taguchi, T. Yokoyama, and Y. Tanaka, Phys. Rev. B **89**, 085407 (2014).

[42] S. Murakami, N. Nagaosa, and S. C. Zhang, Science **301**, 1348 (2003).

[43] J. Sinova, D. Culcer, Q. Niu, N. A. Sinitsyn, T. Jungwirth, and A. H. MacDonald, Phys. Rev. Lett. **92**, 126603 (2004).

[44] E. I. Rashba, Phys. Rev. B **68**, 241315 (2003).

[45] T. Kimura, Y. Otani, K. Tsukagoshi, and Y. Aoyagi, J. Magn. Magn. Mater. **272-276**, E1333 (2004).

[46] Y. K. Kato, R. C. Myers, A. C. Gossard, and D. D. Awschalom, Science **306**, 1910 (2004).

[47] E. Saitoh, M. Ueda, H. Miyajima, and G. Tatara, Appl. Phys. Lett. **88**, 182509 (2006).